

Vibrating Sample Magnetometry: Analysis and Construction

Syed Alamdar Hussain Shah

Advisors: Dr. Muhammad Sabieh Anwar and Dr. Anzar Khaliq

Department of Physics, Syed Babar Ali School of Science and Engineering, LUMS

Friday, December, 13, 2013

Contents

Introduction	3
1 Magnetic Properties and Their Measurements	4
1.1 Magnetic Properties	4
1.1.1 Classes of Materials	5
1.2 Methods For Measuring Magnetization	6
1.2.1 Extraction Method	7
1.2.2 Alternating (Field) Gradient Magnetometer	8
1.2.3 Vibrating Sample Magnetometer	9
2 Modeling The Vibration Mechanism	11
2.1 Mechanical Vibrator	11
2.1.1 LVDT	12
2.2 Measuring Amplitude of Vibration	14
2.2.1 Curve Fitting for extracting the amplitude of the oscillation	18
2.3 Finding the Electromechanical Transfer Function	20
2.3.1 Basics of a Transfer Function	20
2.3.2 Bode Plots	21
2.3.3 Finding the Frequency Response of the Vibrator	22
3 Modeling the Detection Mechanism	25
3.1 Signal Induced in Detection coils	25
3.2 Selecting a Coil Geometry	27
3.2.1 Closer Look at the Geometric Factors	28

3.2.2	Selecting a Coil Configuration	28
3.3	Magnetization from Induced Voltage	31
4	Construction and Characterization	32
4.1	Construction	32
4.2	Experimentation	36
4.3	Conclusion	41
	Appendix	44

Introduction

This project primarily aims at developing a vibrating sample magnetometer (VSM) for measuring the magnetization of any material sample. Chapter 1 will deal with basic physics and methodology of magnetometry. Different magnetometer schemes are discussed briefly. Special focus is paid to VSM. Chapter 2 gives a detailed analysis on mechanism required for vibrating a physical sample. Chapter 3 outlines details of the detection schemes with different geometries of Faraday coils; where as chapter 4 deals with the lab implementation and some experimental results.

Chapter 1

Magnetic Properties and Their Measurements

1.1 Magnetic Properties

Magnetic field is denoted by \vec{H} , it gives rise to a magnetic induction given by \vec{B} . In free space

$$\vec{B} = \mu_o \vec{H}$$

where μ_o is the permeability of free space. In any medium this relation modifies to

$$\vec{B} = \mu_o \mu_r \vec{H} \quad (1.1)$$

where μ_r is the *relative permeability*. In SI units \vec{H} is measured in Ampere per meter (Am^{-1}), \vec{B} in Tesla (T) and $\mu_o = 4\pi 10^{-7} \text{ Tm/A}$. However in cgs units \vec{B} is given in Gauss (G), \vec{H} in Oersteds (Oe) and μ_o in G/Oe.

In magnetism the most elementary entity is a magnetic dipole, which is defined as two magnetic poles of opposite polarity, separated by some distance. If a dipole has magnetic poles of strength p separated by distance l , then the dipole is said to have a magnetic moment m given by

$$\vec{m} = p\vec{l}. \quad (1.2)$$

When a dipole of moment m is introduced in a magnetic induction B , the magnetic induction tries to align the dipole so that the moment m lies parallel to the induction. The torque experienced by the dipole is simply given by

$$\vec{\tau} = \vec{m} \times \vec{B}$$

or in case of free space

$$\vec{\tau} = \mu_o \vec{m} \times \vec{H}. \quad (1.3)$$

The energy associated with a dipole moment m in the presence of magnetic induction B is given by

$$E = -\vec{m} \cdot \vec{B} \quad (1.4)$$

Since in cgs units B is given in Gauss and E in erg, the magnetic moment m is measured in erg/gauss or emu. However in SI units the magnetic moment is given in Am^2 (Sommerfeld convention).

The magnetic moment is a vector quantity. In a material sample, magnetic moments of a number of dipoles add up to give net magnetic moment. This net magnetic moment per unit volume is called *magnetization* of that material, denoted by M .

$$\vec{M} = \frac{\sum_i \vec{m}_i}{V}. \quad (1.5)$$

Consequently the magnetization is measured in emu/cm^3 in cgs and in A/m in SI.

When a material is placed in an external magnetic field, the applied field tends to align the dipoles present within the material. This leads us to an important property called *susceptibility* of a material which is denoted by χ ,

$$\chi = \frac{M}{H}. \quad (1.6)$$

Increasing the strength of applied field changes the magnetization of sample. However after certain strength, called *saturation magnetization*, the induced magnetization becomes constant.

It is important to note that the χ and the saturation magnetization are bulk properties, i.e., they do not depend on the shape of the material.

1.1.1 Classes of Materials

Depending on susceptibility and other bulk magnetic properties of materials we can classify them as one of the following categories [1].

- *Ferromagnetic*: These materials show a large positive χ . Once magnetization is induced, some of it persists even after the external field is removed.
- *Ferrimagnetic*: These materials are similar to ferromagnetic substances however they have two sublattices which are magnetized in opposite directions. One of the sublattices has a stronger magnetization and hence we are able to see a net magnetization in the material sample.
- *Anti-ferromagnetic*: They are similar to ferrimagnetic materials. However the magnetization of the two opposite sublattices is equal in magnitude. As a result the magnetization of one cancels out that of the other and there is no net magnetization in the material.
- *Paramagnetic*: The atoms or molecules of these materials have a net magnetic moment because the spin and orbital angular momenta of their electrons do not cancel out completely. In the absence of external field they are oriented in random directions. On application of external field they tend to align along it, however due to thermal energy some still stay in random orientation.

This partial alignment produces a small magnetization giving the material a positive χ . The susceptibility of these materials is temperature dependent. When external field is removed, the induced magnetization vanishes.

- *Diamagnetic*: These materials have completely filled electron shells as a result they do not have any dipoles. They tend to cancel the applied magnetic field which gives them a negative χ . However this effect is minute.

There are a number of methods and instruments for measuring magnetization or magnetic susceptibility of a material sample. A few of them are discussed next.

1.2 Methods For Measuring Magnetization

Magnetization and magnetic susceptibility can be measured directly or indirectly by observing any other physical quantities related to these two. Accordingly the instruments for measuring these two parameters employ different techniques. They are broadly categorized into following classes:

- *Induction methods*: In these methods voltage generated through electromagnetic induction is monitored to find the magnetic flux change in a particular coil geometry. This in turn provides the change in value of magnetic induction, which can be used to find the magnetization of different materials. This method is employed in vibrating coil magnetometer, vibrating sample magnetometer, fluxgate magnetometer and extraction magnetometer etc. A few of these will be discussed in detail later.
- *Force methods*: These methods observe the force on a magnetic dipole or a material sample to find the magnetic properties of that material. Examples include torque magnetometers, in which the torque on a magnetic dipole by an external field is measure to find the magnetic moment of the dipole [5]. In a similar method we introduce the material sample in a field with constant gradient and measure the force exerted on the sample using an analytic balance. This can be used to find the magnetization of the sample. Another important implementation of force methods is alternating gradient force magnetometer, which is discussed in detail later.
- *Magneto-optic methods*: These methods make use of changes in optical properties of media under the action of an external magnetic field to determine the field strength and ultimately calculate magnetization. Faraday effect and Kerr effect are the most widely used phenomenons in magneto-optic methods.
- *Electrical methods*: Certain materials exhibit change in electrical properties when introduced inside a magnetic field. These are put to use in, for example, the Hall effect magnetometer. It measures the magnetic field by measuring the hall voltage produced with in the sample by it. This measurement is then used to find magnetization. Similarly magnetostrictive devices deploy materials which change their lengths according to the applied magnetic field.

Finally Magnetoresistive devices compute the applied magnetic field using materials that change their resistance in accordance with the field [1][5].

Some of these schemes are discussed in detail next.

1.2.1 Extraction Method

In this method the sample is inserted in a conducting coil called a ‘search coil’. Both coil and sample are then placed inside a solenoid. The method is based on flux change in search coil when sample is extracted from the coil, or both coil and sample together are removed from the magnetic field of solenoid.

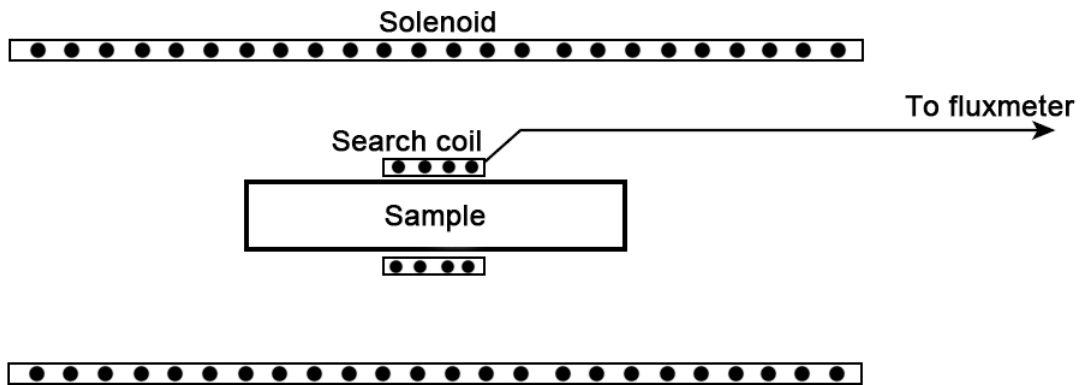


Figure 1.1: Scheme for measuring magnetization using extraction method. The sample is removed from coil and resulting flux change in coil is used for finding magnetization.

Flux through a search coil of crosssectional area A , before removing the sample is

$$\phi_1 = (H + 4\pi M)A \quad (\text{cgs})$$

or

$$\phi_1 = \mu_o(H + M)A \quad (\text{SI}) \quad (1.7)$$

and after removing sample the flux reduces to

$$\phi_2 = HA \quad (\text{cgs})$$

or

$$\phi_2 = \mu_oHA \quad (\text{SI})$$

The fluxmeter measures this change in flux using the voltage induced by it in the search coil. Since

$$v = -N \frac{d\phi}{dt}$$

where v is the induced voltage and N is the number of turns in the search coil, the flux change is given by

$$\Delta\phi = -\frac{1}{N} \int dt.$$

Using equation 1.7 this can be utilized to measure the magnetization of the sample.

1.2.2 Alternating (Field) Gradient Magnetometer

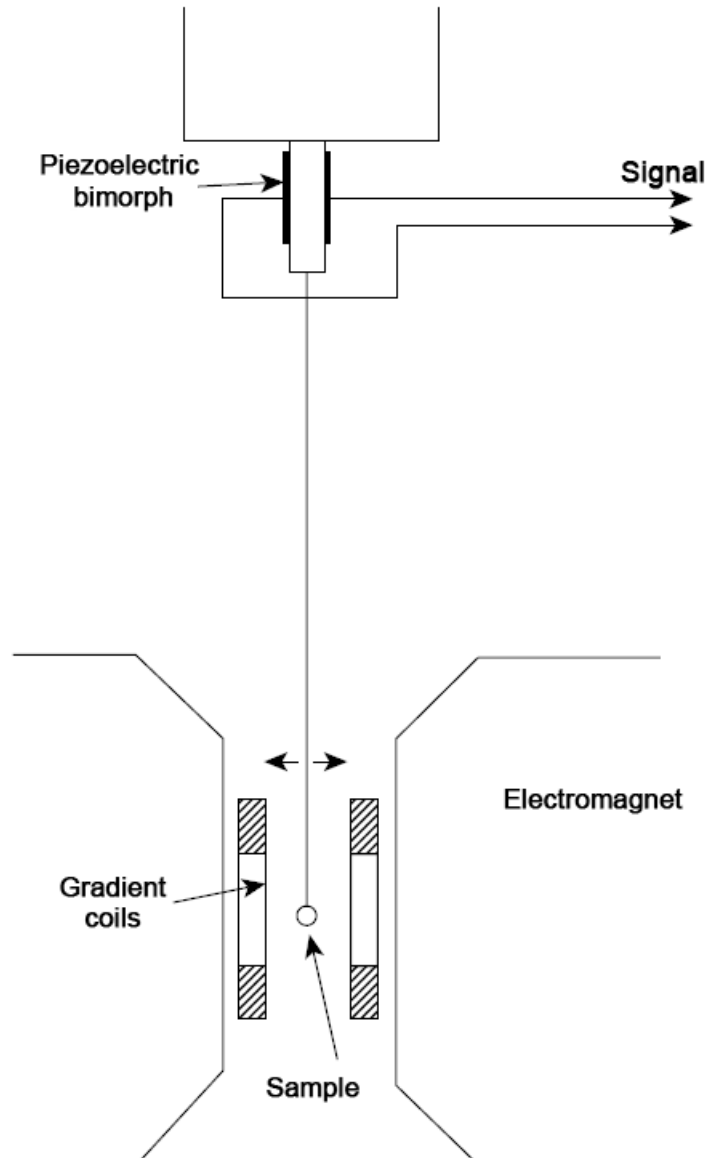


Figure 1.2: Illustration of an alternating gradient magnetometer

In this technique the sample is mounted at the end of a fiber and then subject to a fixed (dc) field plus an alternating field gradient, produced by an appropriate coil pair, as indicated in Figure 1.2. The field gradient produces an alternating force on sample, which causes it to oscillate, flexing the fiber. If frequency of vibration is

tuned to a resonant frequency of the system, the amplitude of vibration increases by a factor equal to quality factor Q of the vibrating system, which can be of the order of 100 [1].

To measure the amplitude of vibration of the fiber an optical microscope can be used. A piezoelectric material can also be utilized for measuring vibrational amplitude. It generates an electrical voltage which is proportional to the amplitude of vibration which in turn is proportional to the magnetic moment and the magnetization of the sample.

However there are a few complications involved. This method is very sensitive to the mass of the sample. Furthermore the presence of a necessary gradient field means that the sample is never in a uniform magnetic field which can be problematic for large samples as induced magnetization will not be uniform.

1.2.3 Vibrating Sample Magnetometer

The vibrating sample magnetometer (VSM) is one of the most successful implementations of a magnetometer. In comparison with alternating gradient magnetometer, the VSM is indifferent to mass and size of sample up to a considerable range. In this scheme the sample is introduced in a constant uniform external magnetic field which induces a magnetisation in the sample. As the magnetized sample is then vibrated, it introduces perturbations in the external magnetic field. A set of coils or some magnetic field sensors can be arranged around the sample to measure these perturbations. For example in the case of coils, magnetic flux piercing the coils will change resulting in generation of an emf (electro motive force) in coils. For a particular coil geometry, the emf generated in coils will depend on (a) the amplitude and frequency of vibration, (b) external magnetic field and (c) the magnetization of sample. With proper manipulation, we can deduce the value for magnetisation from emf. A schematic for VSM is shown in figure 1.3

The project aims at analyzing and developing a VSM that can measure the magnetic susceptibility, at room temperature, of magnetic nanostructured samples.

For this scheme the first crucial step is construction of a vibrating mechanism which can vibrate the sample with measurable and controllable amplitude. Then we need an electromagnet to provide the magnetic field required to magnetise the sample. Finally detection coils are required to detect the magnetic field perturbations produced by vibrating the magnetised sample in the applied magnetic field.

The next chapter will deal with the modeling and construction of this mechanism. It starts with construction of vibration mechanism, subsequently the technique used to measure amplitude of oscillations is described.

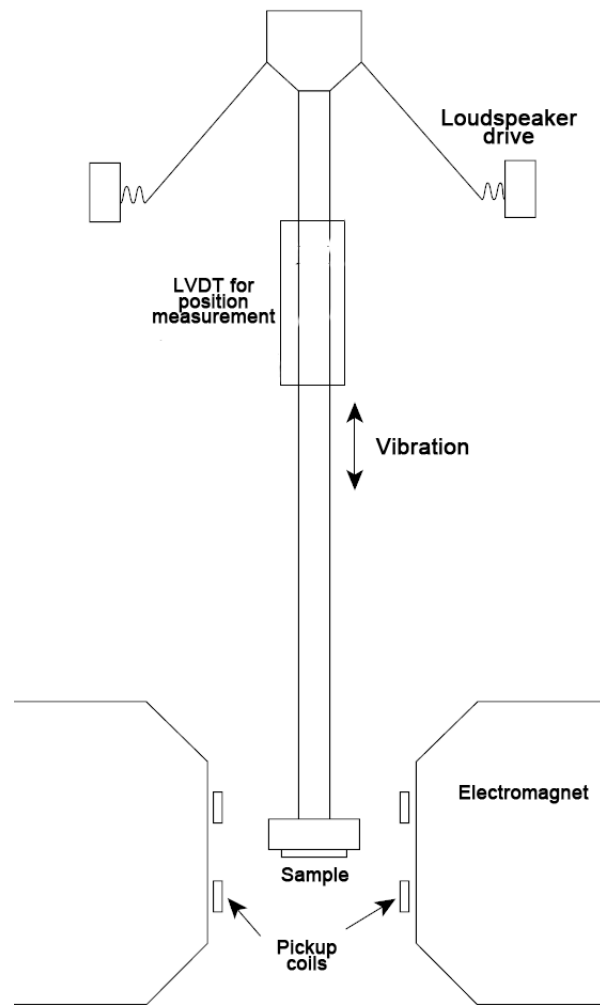


Figure 1.3: Vibrating Sample Magnetometer (schematic).

Chapter 2

Modeling The Vibration Mechanism

The need for a suitable vibration mechanism for VSM cannot be understated. Since we need to vibrate the sample as well as measure the amplitude of vibration, we require a vibration mechanism and an amplitude measuring scheme. This chapter will deal with the construction and analysis of a vibration mechanics. It starts with description of laboratory implementation of the vibrator, afterwards mathematical and computational details of amplitude measuring process are discussed. If we can work out an analytic formula which can give us the amplitude of vibration at any frequency then we can eliminate the need for amplitude measuring instrumentation altogether and rely on a calibration of displacement against the vibrating amplitude. Therefore this chapter will conclude with the calculation of a transfer function that gives amplitude of vibration at any frequency.

2.1 Mechanical Vibrator

In our setup, mechanical oscillations are achieved by a mechanical wave driver (SF-9324 by PASCO), which can be driven within a frequency range of 0.1 Hz to 5000 Hz with amplitudes up to 7 mm. To drive this vibrator we have provided a sine wave excitation signal with 5 V amplitude from a signal generator. This signal alone does not have enough power to drive the vibrator. To obtain the required power, it is first fed into a power amplifier and then supplied to the vibrator. The vibrator is mounted vertically such that it is able to provide oscillations along the vertical axis. Since the materials used in vibrator are magnetic and we need to extend the sample into magnetic field, an aluminium shaft is utilized. It is connected to vibrator from one end and the sample is mounted to the other end. As aluminium is non magnetic, this shaft makes it possible to safely extend the sample into the magnetic field.

The schematic and lab implementations of vibration mechanism are shown in figure 2.1.

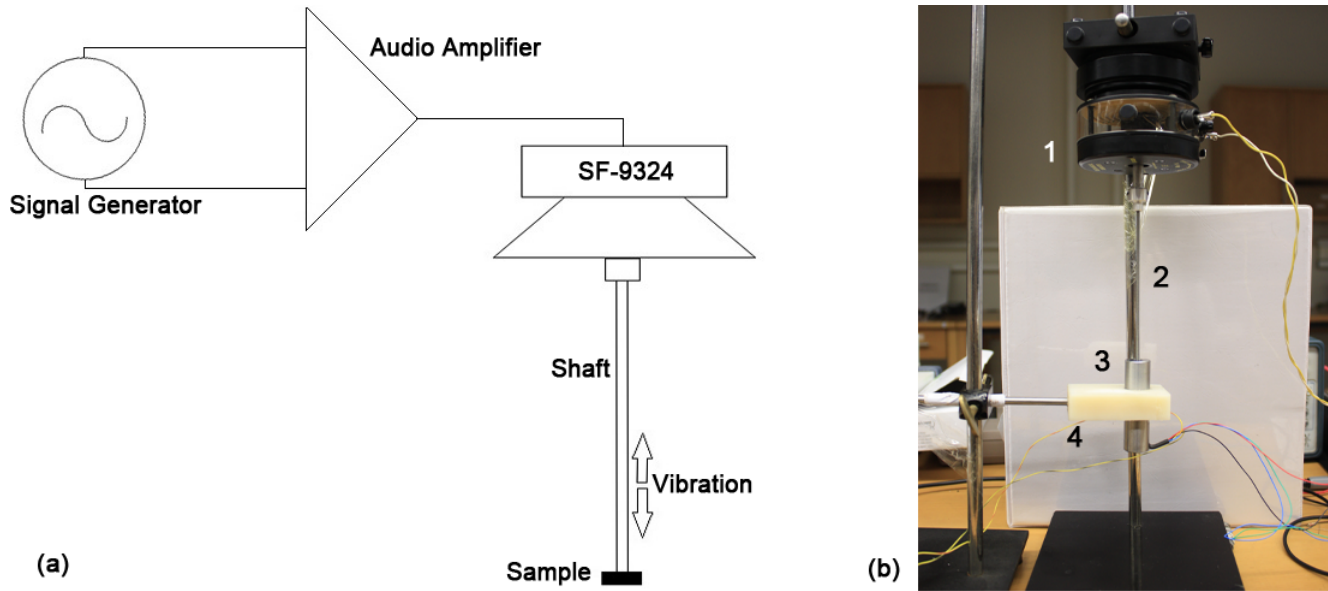


Figure 2.1: (a) Mechanical vibrator system schematic (b) Lab implementation showing the 1 Mechanical wave driver, 2 Shaft, 3 LVDT and 4 Teflon holder for LVDT.

The first step is determining the amplitude of vibration for calculating the magnetization of the sample. For this purpose a linear variable differential transformer (LVDT) is used. Details on the working of LVDT are discussed next.

2.1.1 LVDT

The LVDT is utilised for making precise measurements of linear mechanical displacement of objects in different applications. It consists of one primary and two secondary coils and a moveable core (figure 2.2). The primary is centered inbetween the secondaries and within these coils a magnetically permeable core moves to provide variable coupling between the primary and the secondary coils. The sense of winding in one secondary coil is opposite to that of the other. The secondaries are connected in electrical series. When core is positioned such that there is equal inductive coupling of two secondaries with primary, then emf generated in one secondary cancels that generated in the other. This position of the core is called the ‘Null Point’. As the core moves away from the null point, the inductive coupling of one of the coil becomes larger than the other. Consequently a net emf can be observed across the two secondaries. This emf generated in secondaries is now proportional to position of core and is a function of voltage used to excite the primary coil and the position of core [2]. This brings us to another important property of a LVDT, the ‘sensitivity’ S , which is defined as the induced voltage in millivolts across the secondaries per volt of primary coil excitation per millimeter core displacement.

If a sinusoidal excitation is used for the LVDT’s primary coil then the voltage for primary coil V_p is given by

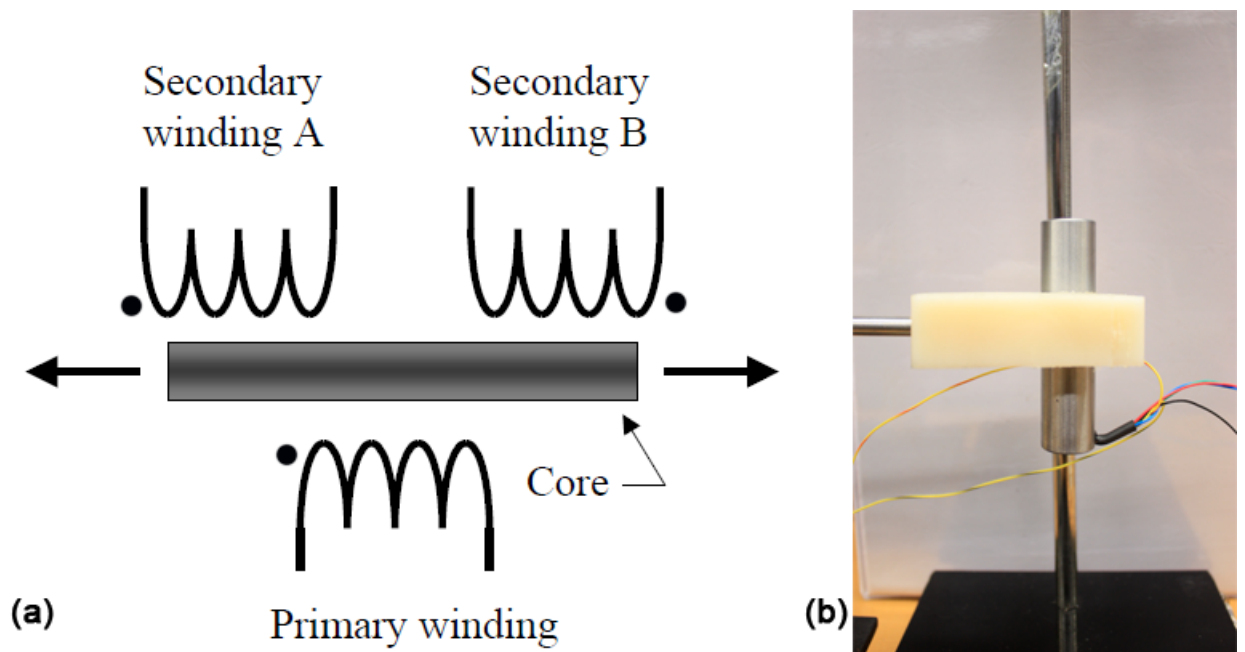


Figure 2.2: (a) Primary and Secondary coils of LVDT. The dots represent sense of winding. (b) LVDT held by a teflon holder.

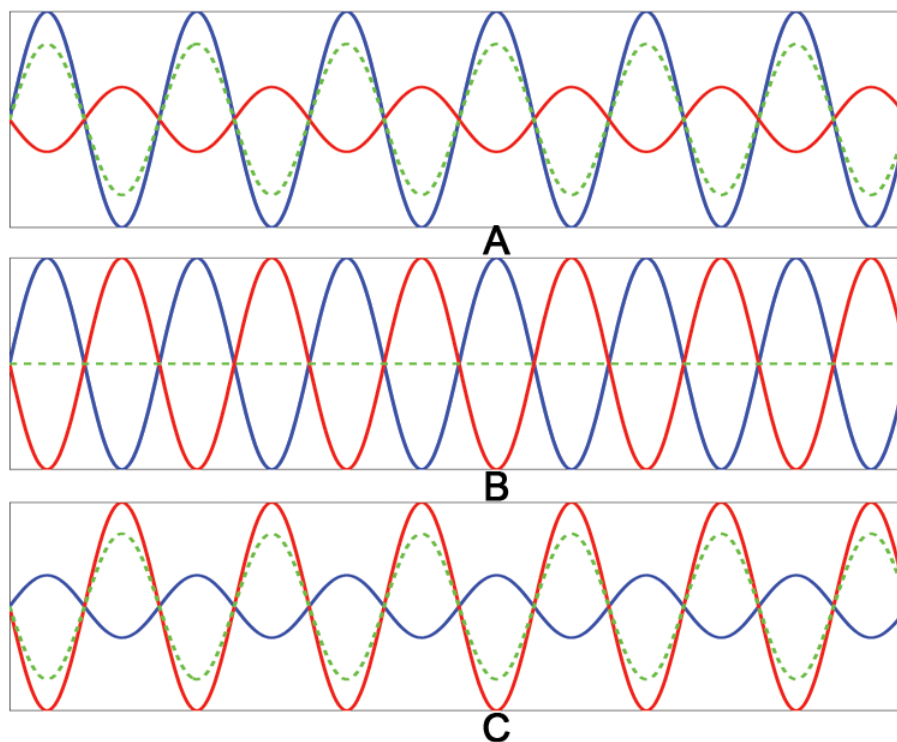


Figure 2.3: Secondary coil voltage for core placed at (A) left (B) null and (C) right positions. The blue and red lines represents V_{S1} and V_{S2} respectively. The dashed green line shows sum of the two voltages according to equation 2.1.

$$V_p = A_p \sin(\omega_L t)$$

where A_p is the amplitude and ω_L is the frequency, the L represents LVDT excitation. Let the two secondary coils be represented as S1 and S2 then the voltages induced in these will be given by

$$V_{S1} = A_{S1} \sin(\omega_L t + \phi_{S1})$$

and

$$V_{S2} = A_{S2} \sin(\omega_L t + \phi_{S2})$$

where ϕ_{S1} and ϕ_{S2} are the phase shifts of the secondary coils with respect to the primary and A_{S1} and A_{S2} are amplitudes of induced voltages in these two coils. These amplitudes are linear functions of core's position provided the core is placed within a range, specific for each LVDT, around the null point. This range is called the 'stroke range' of the LVDT. The graphs of voltages induced in the secondaries are shown in figure 2.3. Since the sense of winding in one secondary is opposite to that in the other, the induced voltages are 180° out of phase with each other and we can write

$$\phi_{S2} = \phi_{S1} + \pi.$$

Let $\phi_{S1} = \phi_L$ then $\phi_{S2} = \phi_L + \pi$. If the secondaries are connected in series then the core's position will simply depend on the difference of A_{S1} and A_{S2} . The emf induced across secondaries will be

$$\begin{aligned} V_S &= V_{S1} + V_{S2} \\ &= (A_{S1} - A_{S2}) \sin(\omega_L t + \phi_L) \end{aligned}$$

Let $A_{S1} - A_{S2}$ be A_S then

$$V_S = A_S \sin(\omega_L t + \phi_L), \quad (2.1)$$

which is the voltage observed across secondaries for some fixed core position. If the core is displaced within the stroke range, then A_S can be written (in linear regime as)

$$A_S = A_0 x \quad (2.2)$$

where x is the displacement of the core from the null point and A is a constant which is determined by the sensitivity and primary coil excitation voltage of the LVDT. For $x = 0$, $A_S = 0$ and for $x = \pm 1$, $A_S = \pm A_0$.

The next section deals with details of how an LVDT was specifically employed in our construction to measure the amplitude of vibration for the oscillations of vibrator. The final goal was to calibrate the magnitude of oscillation as a function of the excitation voltage.

2.2 Measuring Amplitude of Vibration

Since the vibrator was mounted vertically to provide oscillations along vertical axis, the LVDT (E300 by Schaevitz Sensors) was also aligned along the vertical

axis using a homemade teflon holder (Figure 2.2b). The LVDT had a sensitivity of 47.2 mV/V/mm and a stroke range of 7.62 mm. The LVDT's core was attached to the vibrator using a non-magnetic shaft which was attached to the vibrator and the LVDT core by m 3 threading. It was then positioned at the null point. The position of the core is measurable only if it stays at the same point until the voltage induced in the secondaries reaches its maximum value because we are using the amplitude of this voltage for calculating the displacement [2]. It is therefore recommended to have a primary coil excitation frequency which is 10 times the mechanical frequency of the core [2]. We are interested in measuring amplitude for vibrations which themselves have a frequency around 100 Hz, therefore the primary coil of the LVDT was driven using a sinusoidal voltage of 5 V amplitude at 1000 Hz from the signal generator.

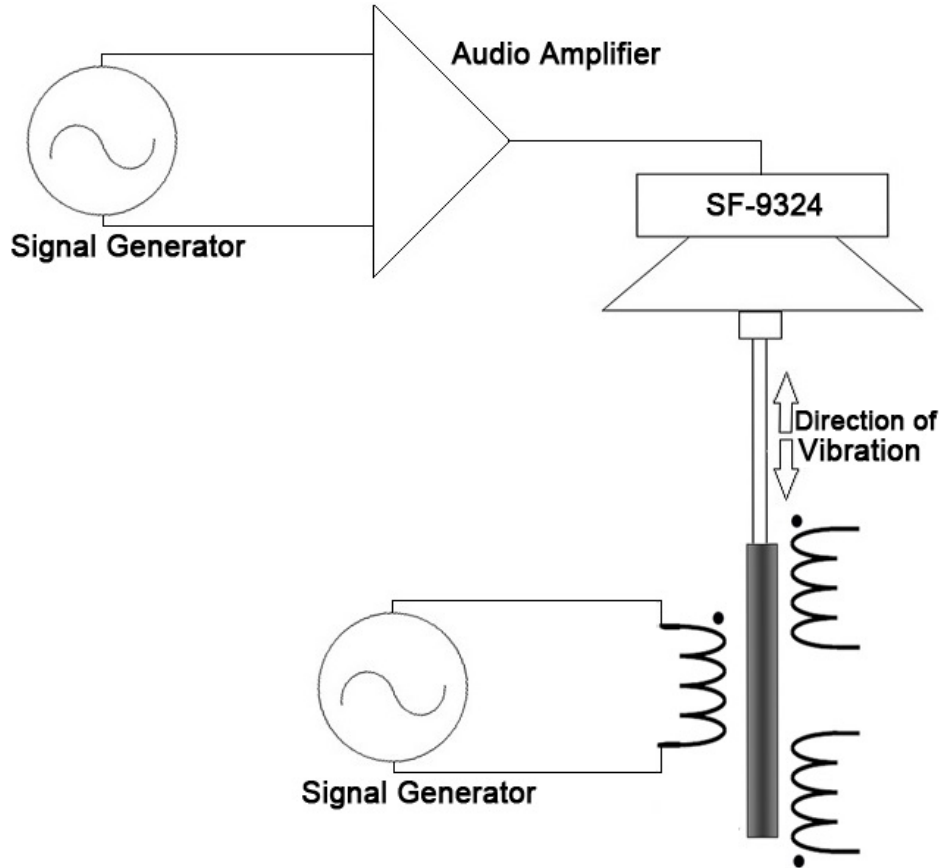


Figure 2.4: Amplitude measurement of the vibrator using an LVDT

When the vibrator was turned on, the core started to oscillate. Suppose the frequency of oscillation was ω_0 (note that this frequency is distinct from ω_L) then the position of the core is approximately given by

$$x = d \sin(\omega_0 t + \phi_0) \quad (2.3)$$

where d is the amplitude and ϕ_0 is the phase of oscillation of the core with respect to some reference. Consequently from (2.1), (2.2) and (2.3), the voltage across

secondaries becomes

$$V_S = Ad \sin(\omega_0 t + \phi_0) \sin(\omega_L t + \phi_L)$$

$$V_S = \frac{Ad}{2} [\cos((\omega_L - \omega_0)t + (\phi_L - \phi_0)) - \cos((\omega_L + \omega_0)t + (\phi_L + \phi_0))]. \quad (2.4)$$

Figure 2.5 shows a simulation for V_S which suggests that this is a beat like pattern with a carrier frequency of $\omega_L + \omega_0$ and an envelope of $\omega_L - \omega_0$. Furthermore the phase shifts do not have any effect on the overall pattern.

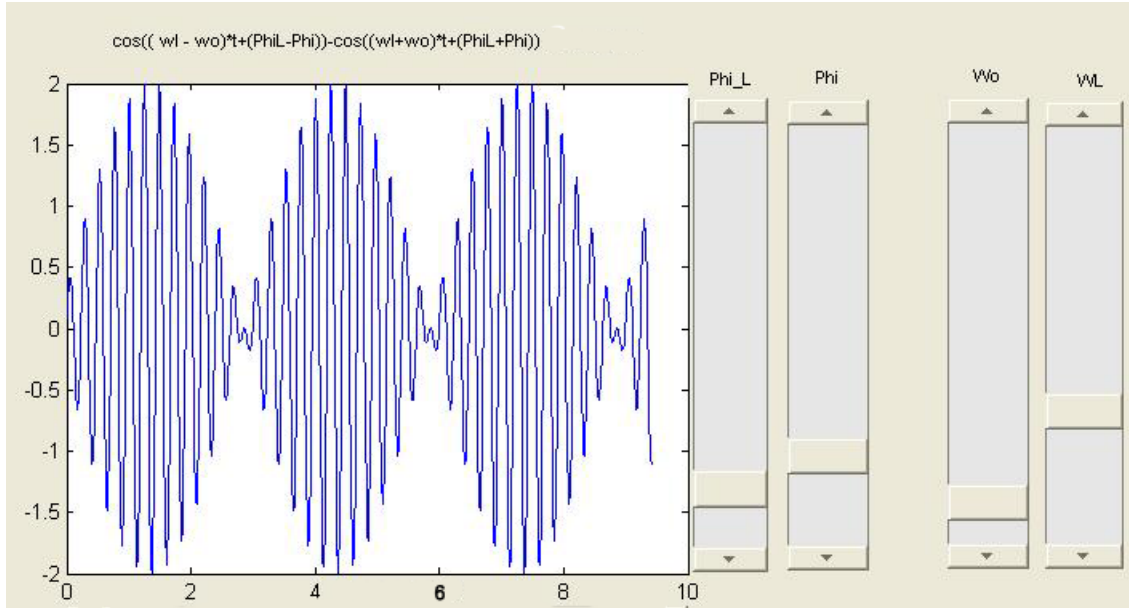


Figure 2.5: A simulation showing waveform of equation 1. The Matlab code file simulation.m is given in the appendix.

It was observed that the voltage from the secondary coils was too small to be measured directly. Therefore it was amplified using an instrumentation amplifier (AD624) since it provides a very broad range of gain and has low input noise. The amplifier's pin connections are shown in figure 2.6. The gain G of the amplifier is given by

$$G = \frac{40000}{R} + 1\Omega$$

By fixing the value of the resistor R (Figure 2.6) the amplifier was calibrated to provide a gain of 6.5.

The amplified voltage was then observed and recorded in LabView using a data acquisition card (DAQ) NI USB 6229. Figure 2.7 shows the schematic for this setup. A block diagram of the LabView file 'data collector' used to measure the amplified voltage is shown in figure 2.8. A high pass filter with a cutoff frequency of 100 Hz is used to remove any low frequency noise signals and an offset introduced by the AD628 amplifier. The filtered data was saved in a file.

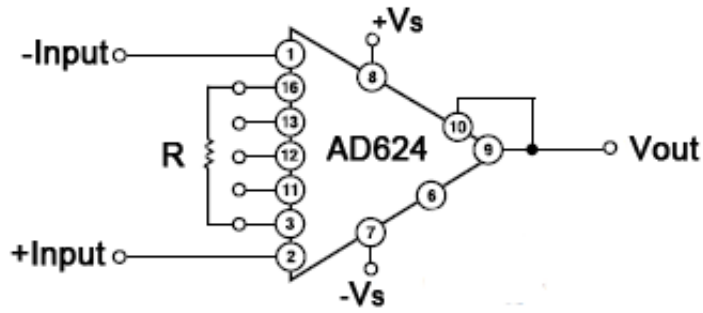


Figure 2.6: Pin connections of the instrumentation amplifier AD624.

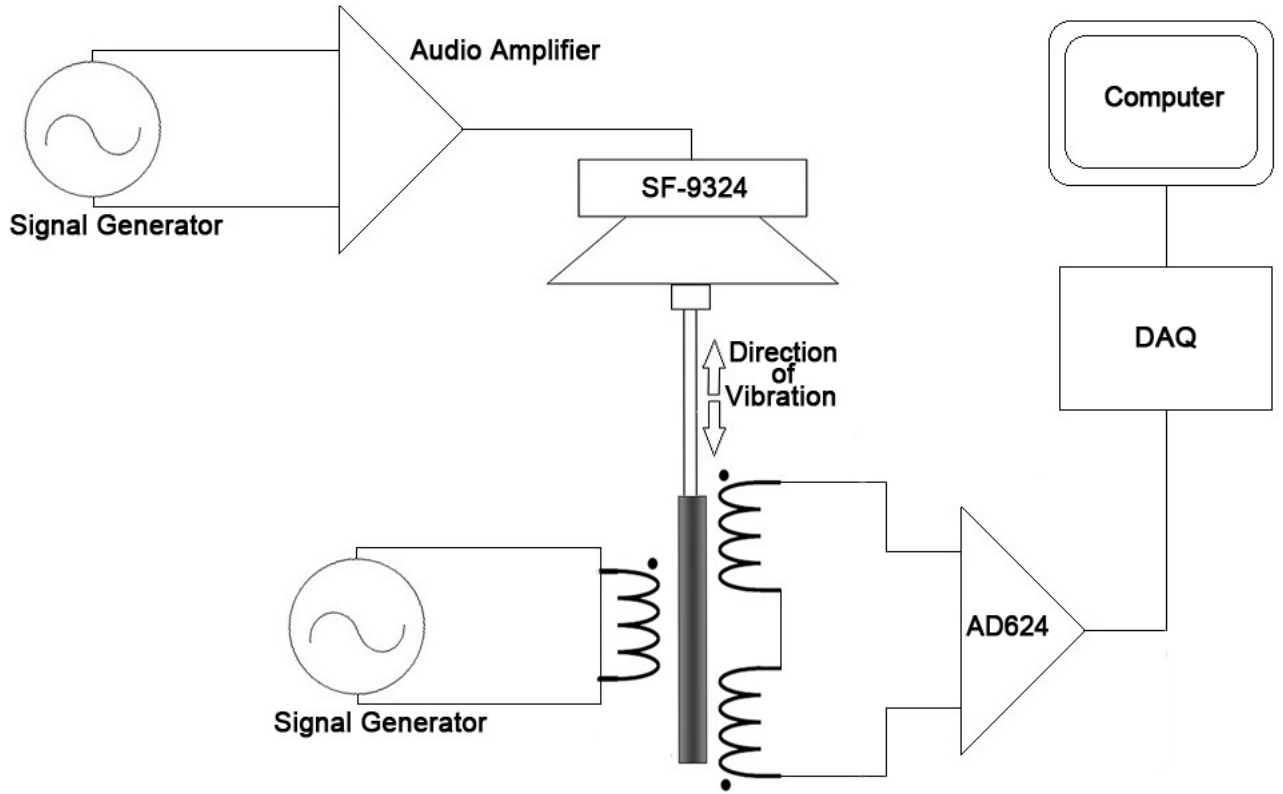


Figure 2.7: Complete setup showing vibration mechanism and amplitude measuring system

The data showed the presence of harmonics in addition to $\omega_L - \omega_0$ and $\omega_L + \omega_0$ (Figure 2.9). In order to obtain meaningful information from the signal, it was exported to Matlab, where curve fitting was utilized to identify as well as quantitatively measure the presence of each harmonic in the signal.

With a primary LVDT voltage $V_L = 5$ V, $S = 47.2$ mV/V/mm and an amplifier gain $G_{amp} = 6.5$, A_0 is predicted to be

$$\begin{aligned} A_0 &= 6.5 \times 5 \times 47.2 \\ &= 1.534 \text{ V/mm.} \end{aligned}$$

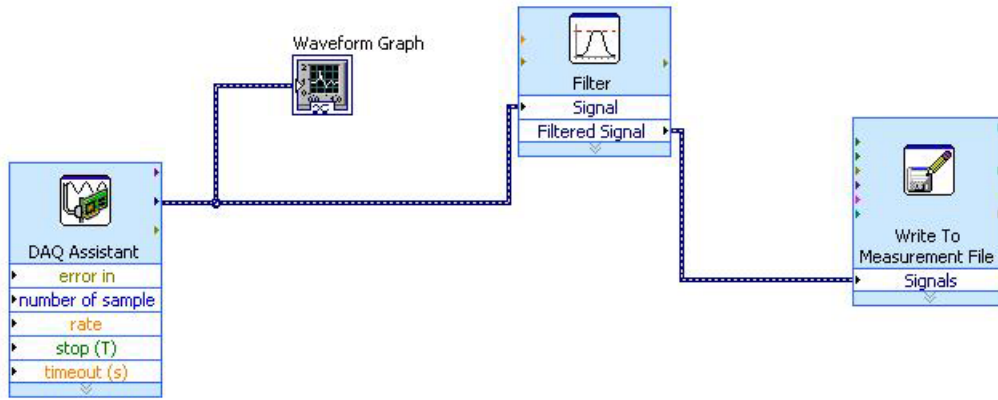


Figure 2.8: LabView File used for inputting LVDT signal readings.

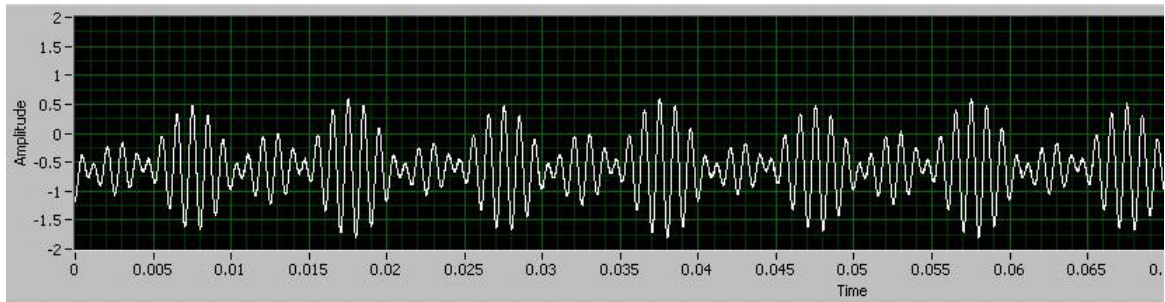


Figure 2.9: Example of LVDT signal amplified by AD628. This signal is to be compared with the simulated signal shown in Fig. 2.5.

In order to get an independent experimental confirmation of the above calculated value for A_0 , the core was mounted on a translation stage fitted with a micrometer screw gauge. The amplitude of V_S ($|V_S|$) was given by LabView and precise displacement of core was observed from translation stage. Then using $|V_S| = Ad$, A was calculated to be 1.52 V/mm, in good agreement with the value of 1.53 V/mm. This means that an output voltage of 1.53 V corresponds to a displacement of 1 mm. All displacements can thus be measured against this calibration factor.

The next section elaborates the details of curve fitting for calculating the amplitude of mechanical oscillations of the core and also recounts a brief introduction of curve fitting toolbox in Matlab.

2.2.1 Curve Fitting for extracting the amplitude of the oscillation

As pointed out earlier the signal recorded by LabView showed presence of harmonics in addition to those predicted by equation 2.4. The recorded signal was imported in Matlab and 'Curve fitting toolbox' was utilized to get a mathematical

expression for it [6]. The curve fitting toolbox provides a number of mathematical expressions and methods for curve fitting. The graphic interface for this toolbox is shown in figure 2.10. ‘X data’ and ‘Y data’ represent the independent and de-

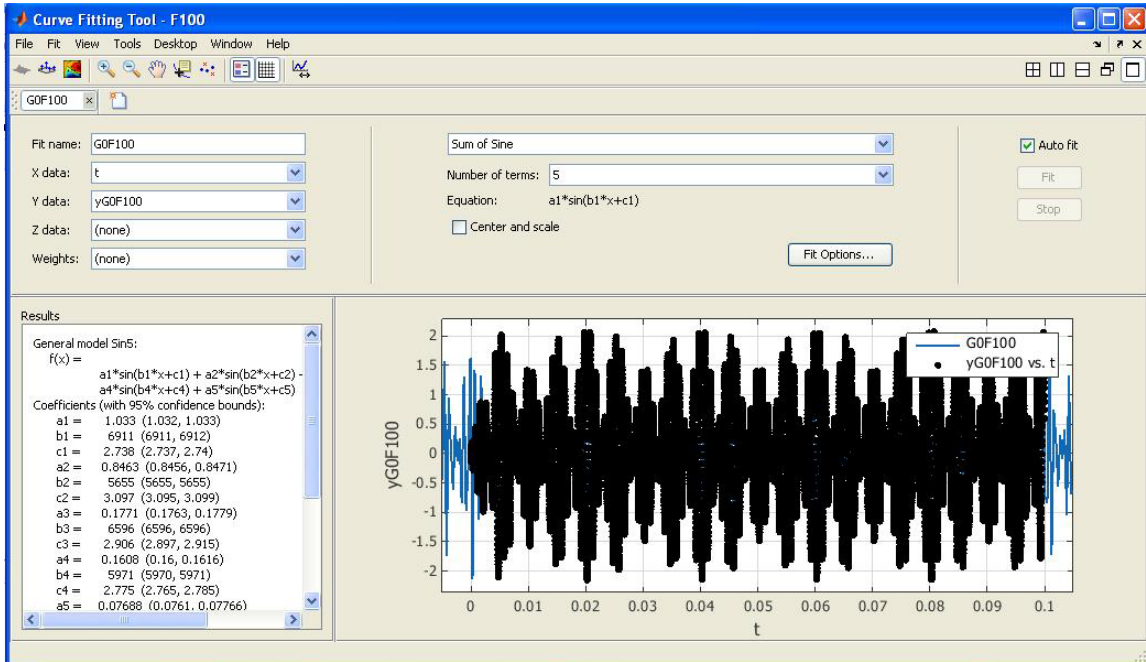


Figure 2.10: Curve Fitting Tool Box used for analysing the LVDT signal

pendent variables respectively. The type of mathematical expression we want to curve fit is selected from the dropdown menu located at upper central portion of graphic interface as shown in figure 2.10.

As equation 2.4 predicts, a ‘sum of sine’ curve was selected for curve fitting the recorded signal. The results gave different harmonics, their coefficients and phases with 95% confidence. The waveform was fit for five unknowns. The two harmonics $\omega_L \pm \omega_0$ appear in equation 2.4 duly appear in the LVDT signal. The other harmonics were $\omega_L \pm (2\pi \times 50)$ and ω_L and the raw 50 Hz is from electromagnetic interference (line noise). The origin of ω_L is due to the fact that it is difficult to position the core at exact null point to begin with, causing the LVDT excitation frequency ω_L to leak through. Hence we can correctly identify the various harmonics present in the signal, the desired ($\omega_L \pm \omega_0$) terms as well as the interference terms.

The coefficients of $\omega_L - \omega_0$ (difference) and $\omega_L + \omega_0$ (sum) terms are obtained from curve fitting. Ideally, from equation 2.4 both coefficients should be equal to $Ad/2$, the amplitude of V_S . However curve fitting results showed that the one for ‘sum’ term, A_{sum} , was greater than that for the ‘difference’ term, A_{diff} . To get the amplitude of vibration in millimeters, an average of these two coefficients was utilized. Let this average be A_{avg} then

$$A_{avg} = \frac{Ad}{2}$$

$$d = \frac{2A_{avg}}{1.53} \text{ mm} = 1.31A_{avg} \text{ mm} \quad (2.5)$$

which gives us the amplitude of mechanical oscillation for the vibrator in terms of the measured signal from the LVDT.

We have finally utilized the electrical signal obtained from the LVDT to measure the amplitude of mechanical vibration. By converting A_{avg} to d we now have a scheme to find the amplitude of mechanical oscillations using LVDT. However if, based on these displacement measurements, we can formulate a mathematical model for the vibrator then we can eliminate the requirement of the LVDT altogether. We can simply use that formula to find the amplitude of mechanical vibration at any mechanical frequencies and driving amplitude of the vibrator.

Mathematical modeling can be done in a number of ways, one of them is by finding the ‘transfer function’ which will be defined in the next section. Furthermore a transfer function will be experimentally determined for the vibrator. The transfer function relates the strength of the mechanical to the electronic input provided by the function generator.

2.3 Finding the Electromechanical Transfer Function

2.3.1 Basics of a Transfer Function

A transfer function is the ratio of the output of a system to its input, generally expressed in Laplace or Fourier domain. For example, suppose we give an input u to a physical process and obtain an output v . Let the Laplace transform of u and v be U and V respectively. Then the ratio V/U , representing the physical process is called the transfer function for the process. The transfer function captures the frequency response of the system as well.

Conversely if we know the transfer function of a physical process we can find the temporal mathematical expression governing it by simply taking its inverse transform. Finding a differential equation may become difficult for complicated processes. We can determine their transfer function, for example, by observing their response to sinusoidal inputs, a step or impulse inputs etc. Response to different input frequencies is observed and the frequency response or transfer function is built up. This procedure is called system identification.

As explained earlier, a sinusoidal signal was generated by the function generator, amplified by an audio amplifier and then fed to the mechanical oscillator. The amplitude of mechanical vibrations depends on the amplitude and frequency of the sinusoidal signal generated by the function generator. To obtain an analytic function that can give us the mechanical oscillation amplitude at any frequency, we first calculated the frequency response by driving the mechanical oscillator at

different frequencies and then calculating the resulting vibrational amplitudes. We then drew the Bode plots from which the transfer function was estimated.

2.3.2 Bode Plots

If a mathematical function consists of product of different expressions then we can take its log and convert the product to sum of log of those expression. This implies that the graph of log of that function will simply be sum of the graphs of the logs of individual expressions or terms. For example suppose a transfer function (or any mathematical function for that matter) with multiple terms is given in polar form as,

$$\begin{aligned} G(\omega) &= \frac{r_1 e^{-i\theta_1} r_2 e^{-i\theta_2}}{r_3 e^{-i\theta_3} r_4 e^{-i\theta_4}} \\ &= \left(\frac{r_1 r_2}{r_3 r_4} \right) e^{-i(\theta_1 + \theta_2 - \theta_3 - \theta_4)} \end{aligned}$$

where r_i 's and θ_i 's are real functions of ω . Since

$$|G(\omega)| = \frac{r_1 r_2}{r_3 r_4},$$

taking log on both sides gives us

$$\log(|G(\omega)|) = \log r_1 + \log r_2 - \log r_3 - \log r_4.$$

This shows that if we plot log of magnitude versus log of frequency ω then contributions from these different terms sum up to give the composite curve. Conversely if we have a composite curve then the transfer function can be calculated by identifying the individual terms. Such a plot with logarithmic axes is known as the 'Bode Plot'.

A transfer function is normally composed of three classes of terms [3]:

1. $K_0(-i\omega)^n$
2. $(1 - i\omega\tau)^{\pm 1}$
3. $[(\frac{-i\omega}{\omega_n})^2 + 2\zeta\frac{-i\omega}{\omega_n} + 1]^{\pm 1}$

where ζ is a damping factor [3]. These three terms can be immediately identified on the Bode plot as follows.

(a) $K_0(-i\omega)^n$ is a straight line on the Bode plot with a slope n because

$$\log (K_0|(-i\omega)^n|) = \log K_0 + n \log |\omega|$$

It passes through $\omega = 1$ at $\log K_0$. Its graph is shown in figure 2.11.

(b) For the second class of terms, $(1 - i\omega\tau) \cong 1$ for $\omega\tau \ll 1$ and $(1 - i\omega\tau) \cong -i\omega\tau$ for $\omega\tau \gg 1$. This shows that the magnitude of this term approaches one

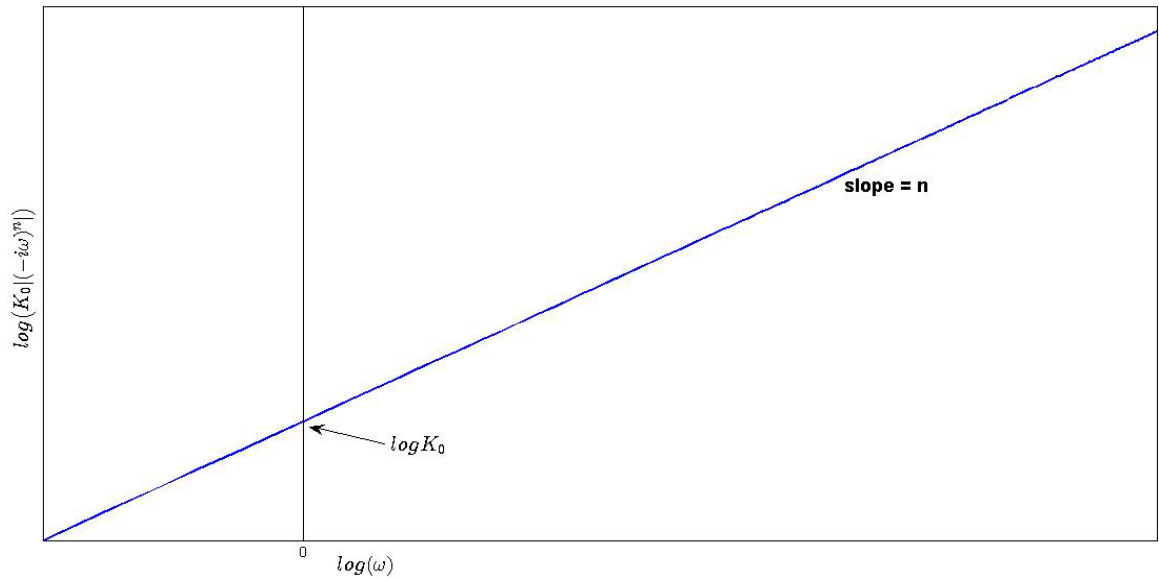


Figure 2.11: Bode plot for a Class 1 term.

asymptote at very low frequencies and another at very high frequencies. Below $\omega = 1/\tau$ it is approximately constant (1), while above this point it behaves as class 1 term. This point is known as the ‘break point’. Due to this term the slope of composite curve will change by 1 at the break point. If slope changes by +1, this term belongs to the numerator and if by -1 , then to the denominator of the transfer function. This term is graphed in figure 2.12.

(c) Finally $[(\frac{-i\omega}{\omega_n})^2 + 2\zeta\frac{-i\omega}{\omega_n} + 1]^{\pm 1}$ behaves almost like class 2 term but with a few notable changes. The break point is now at the natural frequency ω_n and the slope of composite curve is changed by a factor of 2 at the break point due to this term.

2.3.3 Finding the Frequency Response of the Vibrator

For calculating the analytic function for amplitude of mechanical vibrations, the gain of the audio amplifier was set to 1 and mechanical amplitude was measured for a frequency range of 1 to 1000 Hz. The resulting frequency response plot is shown in Figure 2.13. As we move from lower frequencies to higher ones we note our first asymptote which has a slope 2. To find the value for K_0 we look for the value of displacement corresponding to $\omega = 1$ at the asymptote. It turns out to be 1.02.

Next asymptote, with a slope 0, intersects the first one at the break point $\omega = 20$ rad/s. Since the slope changes by -2 , this indicates the presence of a class three term, with natural frequency $\omega_1 = 20$ rad/s, in denominator of the transfer function.

Third and final asymptote with slope $n = -2$, intersects the second one at $\omega = 250$ rad/s. It gives another class three term of natural frequency $\omega_2 = 250$ rad/s for the denominator of the transfer function. As result the transfer function turns out

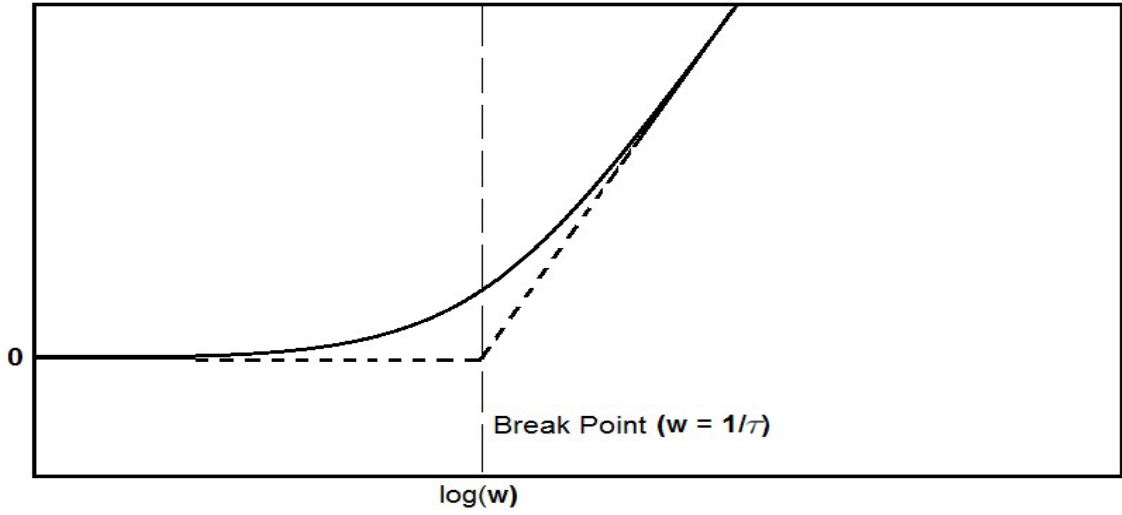


Figure 2.12: Class 2 term logarithmic graph indicating the break point.

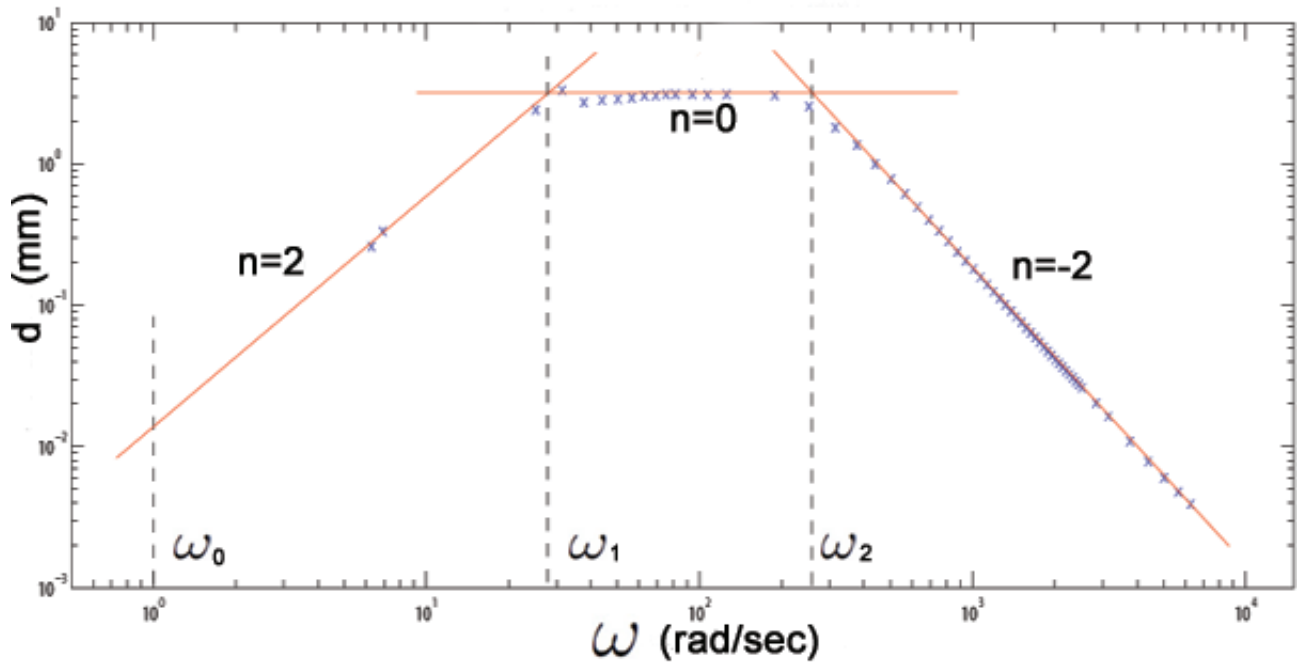


Figure 2.13: The Bode plot for frequency response of the vibrator and the asymptotes are overlaid on top of it. Experimentally determined plots are shown as crosses. The electrical input signal had 5 V amplitude.

to be:

$$|G(\omega)| = |d| = \frac{K_0(\omega i)^2}{[(\frac{i\omega}{\omega_2})^2 + 2\zeta_2 \frac{-i\omega}{\omega_2} + 1][(\frac{i\omega}{\omega_1})^2 + 2\zeta_1 \frac{-i\omega}{\omega_1} + 1]}$$

$$\text{or } |d| = \frac{K_0\omega^2}{\sqrt{(1 - \frac{\omega}{\omega_1})^2 + (2\zeta_1 \frac{\omega}{\omega_1})^2} \sqrt{(1 - \frac{\omega}{\omega_2})^2 + (2\zeta_2 \frac{\omega}{\omega_2})^2}} \text{ mm} \quad (2.6)$$

where $K_0 = 1.02$, $\omega_1 = 20$ rad/sec and $\omega_2 = 250$ rad/sec. The terms ζ_1 and ζ_2

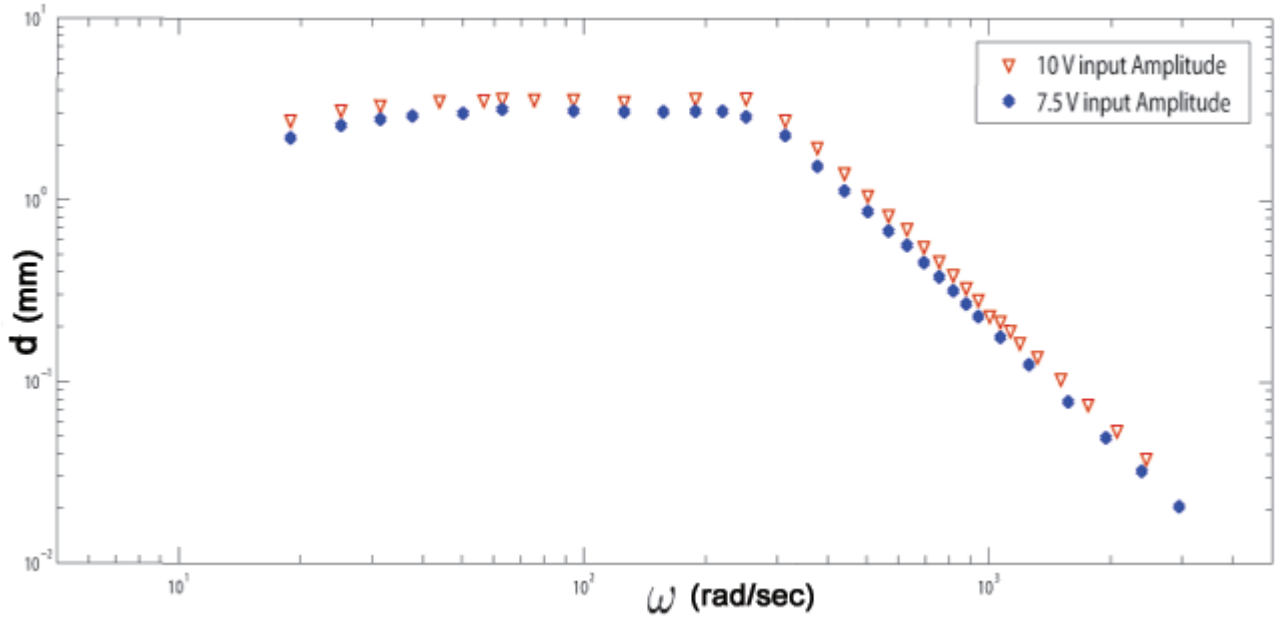


Figure 2.14: Frequency response for 10V and 7.5V input signals.

Table 2.1: Coefficients for the transfer function

Coefficients	5V Amp	7.5V Amp	10V Amp
K_0	0.00654	0.0114	0.0138
ω_1	21.1	18.36	18.00
Ω_2	247.3	268.3	273.9
ζ_1	0.65	0.70	0.66
ζ_2	0.57	0.56	0.52

are damping coefficients which can be determined by curve fitting equation 2.6 on the experimentally determined Bode plot. It is difficult to have more readings for the low frequencies in the Bode plot because we are using a logarithmic scale. Therefore the absolute difference in the consecutive frequency readings decreases exponentially which makes it difficult to generate and observe the mechanical oscillations at these frequencies. Furthermore in the VSM the vibrator was operated around 100 Hz, for which the term generated by the low frequencies in the expression for d , has ignorable effect.

Now we have an analytic function that can give us amplitude of mechanical oscillation at any given frequency. This, however, is applicable to only one mechanical amplitude. We might need different mechanical amplitudes Hence we find the transfer function at varying amplitudes A_m , $G(\omega, A_m)$. Therefore three electrical signals with different amplitudes (5V, 7.5V and 10V) were generated from function generator and frequency response was calculated for each one of them. Figure 2.14 shows frequency response for 10V and 7.5V amplitude input signals. They suggest that equation 2.6 still holds however coefficients in the equation will now be different. The coefficients for all three responses are summarized in table 2.1.

Chapter 3

Modeling the Detection Mechanism

As discussed in chapter 1, in a VSM we vibrate a sample inside an applied magnetic field. The magnetized sample then induces emf in coils placed nearby. These coils are called *detection coils*. To calculate the induced voltage and most favourable placement for the detection coils we first need to find the magnetic field produced by the vibrating sample and then calculate the magnetic flux through the coils. In this chapter we will work out the field produced by the magnetized sample. Afterwards a particular coil arrangement will be selected and the expected emf will be calculated. Finally an expression for extracting magnetization from induced emf will be constructed.

3.1 Signal Induced in Detection coils

Suppose our magnetized sample is placed at the origin. If the position of this sample is varied, sinusoidally, over a small distance $\vec{\delta}(t)$ (figure 3.1) then a change of flux $\partial\vec{B}(t)$ that will be induced at a point \vec{r} in space will be [4]

$$\partial\vec{B}(t) = \mu_0\vec{\delta}(t) \cdot \text{grad}\{\vec{H}(\vec{r})\}. \quad (3.1)$$

If we place a small coil at r then the voltage induced in it will be given by

$$V(t) = \sum_p \sum_n \int_A \left(\frac{\partial\vec{B}}{\partial t}\right) \cdot d\vec{A}, \quad (3.2)$$

where n is the number of turns, A denotes the area vector of a single turn and p is the number of coils (as we can have multiple coils). The summation over n includes only those turns which contain elemental area $d\vec{A}$ and for which $\partial\vec{B}/\partial t$ is given by equation 3.1.

Clearly to proceed any further we need to have an analytic formula for $\vec{H}(\vec{r})$. For this we can approximate our magnetized sample with a magnetic dipole if the

dimensions (size) of our sample are small as compared to the distances between the sample and the detection coils. With this approximation we can assume the vibrating sample to be an oscillating dipole. The magnetic field of a dipole placed at origin is given by [4].

$$\vec{H}(\vec{r}) = \frac{1}{4\pi} \left(\frac{\vec{m}}{r^3} - \frac{3(\vec{m} \cdot \vec{r})\vec{r}}{r^5} \right) \quad (3.3)$$

where \vec{r} is the position vector of a point in space and \vec{m} is the magnetization of the sample. Suppose the sample is vibrated sinusoidally along the z -axis and the external magnetic field is applied along the x -axis as shown in figure ???. Then

$$\vec{\delta}(t) = \sin(\omega_0 t + \phi_0) \vec{d}. \quad (3.4)$$

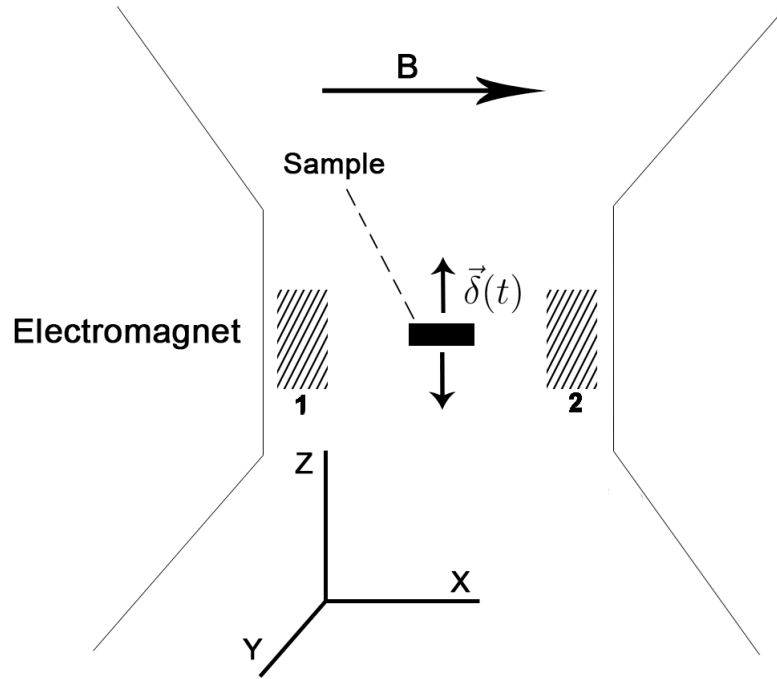


Figure 3.1: A sample oscillated in a magnetic field and vibrated along the z -axis. (1) and (2) are the detection coils.

Furthermore let the magnetic moment of the dipole, polarized along x -axis, be

$$\vec{m} = (m, 0, 0)$$

then the field induced by the sample at the position of a coil \vec{r} will be

$$\begin{aligned} \vec{H}(\vec{r}) &= \frac{1}{4\pi} \left(\frac{(m, 0, 0)}{r^3} - \frac{3((mx))(x, y, z)}{r^5} \right) \\ &= -\frac{1}{4\pi} \left(\frac{-m}{r^3} + \frac{3mx^2}{r^5}, \frac{3mxy}{r^5}, \frac{3mxz}{r^5} \right). \end{aligned}$$

As a result the gradient of $\vec{H}(\vec{r})$ at \vec{r} will be given by

$$\nabla \vec{H}(\vec{r}) = \begin{pmatrix} \frac{\partial \vec{H}}{\partial x} \\ \frac{\partial \vec{H}}{\partial y} \\ \frac{\partial \vec{H}}{\partial z} \end{pmatrix}$$

$$\nabla \vec{H}(\vec{r}) = -\frac{3m}{4\pi r^7} \begin{pmatrix} x(3r^2 - 5x^2) & y(r^2 - 5x^2) & z(r^2 - 5x^2) \\ y(r^2 - 5x^2) & x(r^2 - 5y^2) & -5xyz \\ z(r^2 - 5x^2) & -5xyz & x(r^2 - 5z^2) \end{pmatrix}. \quad (3.5)$$

Then using equation 3.1, 3.4 and 3.5 we obtain

$$\begin{aligned} \frac{\partial \vec{B}}{\partial t} &= \mu_0 \omega_0 \cos(\omega_0 t) \vec{d} \cdot \nabla \vec{H}(\vec{r}) \\ &= -\frac{3m\mu_0\omega_0}{4\pi r^7} \cos(\omega_0 t) d(z(r^2 - 5x^2)\hat{i}, -5xyz\hat{j}, x(r^2 - 5z^2)\hat{k}) \end{aligned}$$

consequently by equation 3.2, we obtain the induced emf,

$$V = -\frac{3}{4\pi} m\mu_0\omega_0 \cos(\omega_0 t) d \sum_n \int_A d\vec{A} \cdot \left(\frac{1}{r^7}\right) (z(r^2 - 5x^2)\hat{i}, -5xyz\hat{j}, x(r^2 - 5z^2)\hat{k}). \quad (3.6)$$

In this equation the direction of the external magnetic field determines the direction of \vec{m} and the orientation of the axis of the coil determines the direction of the area vector $d\vec{A}$. If we increase the size of the coil, the induced voltage would increase but it can be increased only to an extent in which the dipole approximation holds. Otherwise equation 3.6 would be invalid.

3.2 Selecting a Coil Geometry

From inspection of equation 3.6 we can see that by orienting coils along x , y or z axis, we can select any of the orthogonal components (i 'th, j 'th or k 'th) of the flux change $\frac{\partial \vec{B}}{\partial t}$.

For example if a coil is oriented along z -axis then $d\vec{A} = dA\hat{k}$, as a result from equation 3.6

$$V = -\frac{3}{4\pi} m\mu_0\omega_0 \cos(\omega_0 t) d \sum_n \int_A dA \frac{x(r^2 - 5z^2)}{r^7}$$

A closer look shows that the induced voltage crucially depends on the term in the integral. As it is a function of the coil geometry only, we will call it a geometric factor g_z .

$$g_z = \frac{x(r^2 - 5z^2)}{r^7}$$

Similarly geometric factors

$$g_x = \frac{z(r^2 - 5x^2)}{r^7} \text{ and } g_y = \frac{-5xyz}{r^7}$$

dictate the induced voltages in coils oriented along x and y axis respectively. These geometric factors are to be integrated over the pick up area of the coils.

3.2.1 Closer Look at the Geometric Factors

To select a suitable coil configuration it is important to understand the behaviour of geometric factors in the region surrounding the vibrating sample. Particularly we are interested in the contours of these factors. A little manipulation shows that

$$\begin{aligned} g_x(r, \theta, \phi) &= z(r^2 - 5x^2)/r^7 = \cos \theta (1 - 5 \sin^2 \theta \cos^2 \phi)/r^4 \\ g_y(r, \theta, \phi) &= -5xyz/r^7 = -\frac{5}{2} \sin^2 \theta \cos \theta \sin(2\phi)/r^4 \\ g_z(r, \theta, \phi) &= x(r^2 - 5z^2)/r^7 = \sin \theta (1 - 5 \sin^2 \theta) \cos \phi/r^4. \end{aligned}$$

Their contours are shown in figure 3.2 through figure 3.4. It can be seen that for g_x , a change of sign takes place whenever θ passes through $\sin^{-1}(1/\sqrt{5} \cos \phi)$. Similarly g_z changes sign at $\theta = 62^\circ 54'$. However for g_y the sign remains unchanged.

Since

$$V = -\frac{3}{4\pi} m \mu_0 \omega_0 \cos(\omega_0 t) d \sum_n \int_A d\vec{A} \cdot \vec{g}$$

where $\vec{g} = (g_x, g_y, g_z)$, the g 's are the factors which sample space and contribute to the voltage. With coils placed at points dictated by these factors, the induced voltage is predictable.

3.2.2 Selecting a Coil Configuration

The contours indicate that suitable dimensions for a detection coil are one in which the sign of the geometric factor stays the same because otherwise the flux change from regions with opposite signs will cancel each other out. Furthermore the coils oriented along x -axis will also detect any perturbations in the external magnetic field which is an undesired artifact and will unnecessarily complicate the analysis at such an early stage. However coils along y and z axis do not suffer this complication as their cross-sectional area vectors are perpendicular to the external magnetic field. Taking these factors into account, we have selected a coil configuration with two detection coils. These coils will be placed along x -axis, one on each side of the sample and their cross-sectional areas will be oriented along the z -axis. Therefore we need to have a closer look at the behaviour of g_k .

Figure 3.5 shows a complete volume contour for g_k at two values, other values show similar structure. This indicates that if a positive voltage is induced in the coil placed at $+x$ axis then an equal negative voltage is produced in an identical coil

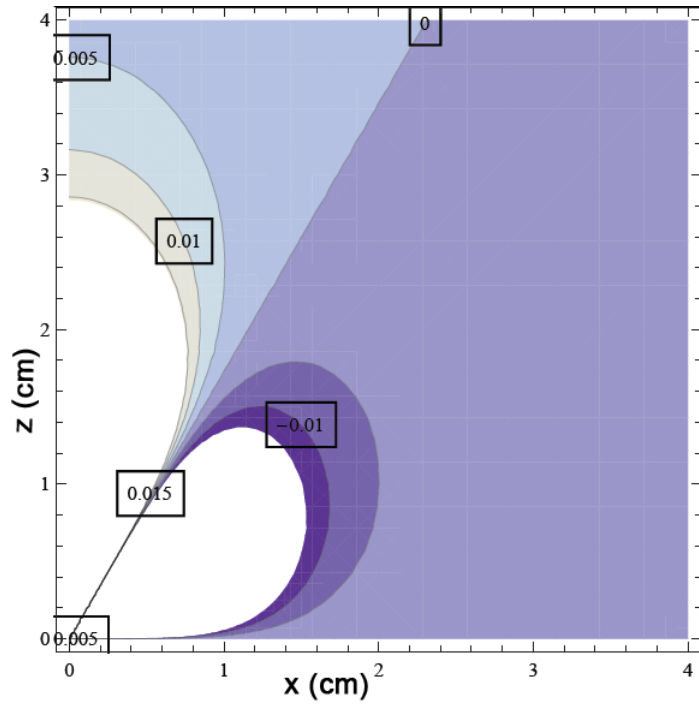


Figure 3.2: Equi-signal contours of g_x for $\phi = 45^\circ$ and $0 \leq \theta \leq 90^\circ$.

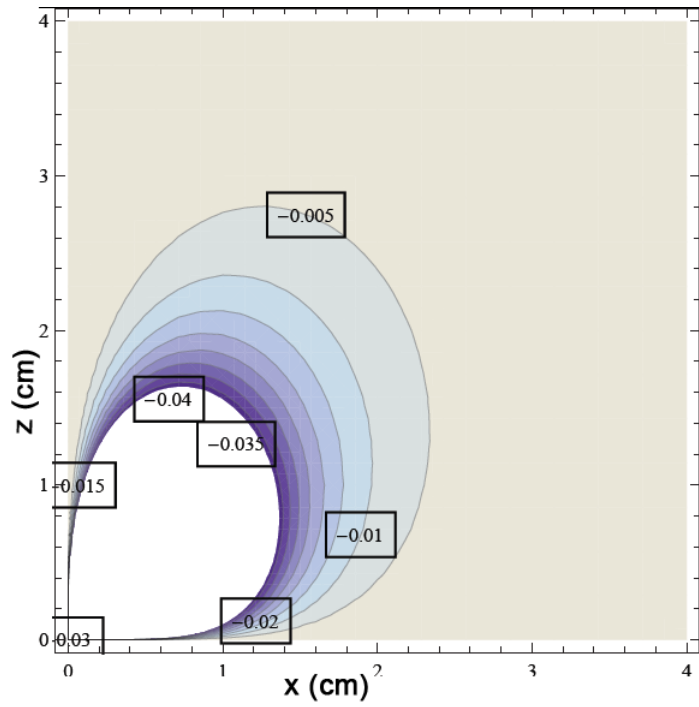


Figure 3.3: g_y equi-signal contours at $\phi = 45^\circ$ and $0 \leq \theta \leq 90^\circ$.

placed at $-x$. Winding one of the coils clockwise and the other anti-clock wise will result in generation of the same signed voltage in both coils. We can then connect them in electrical series to get a stronger signal.

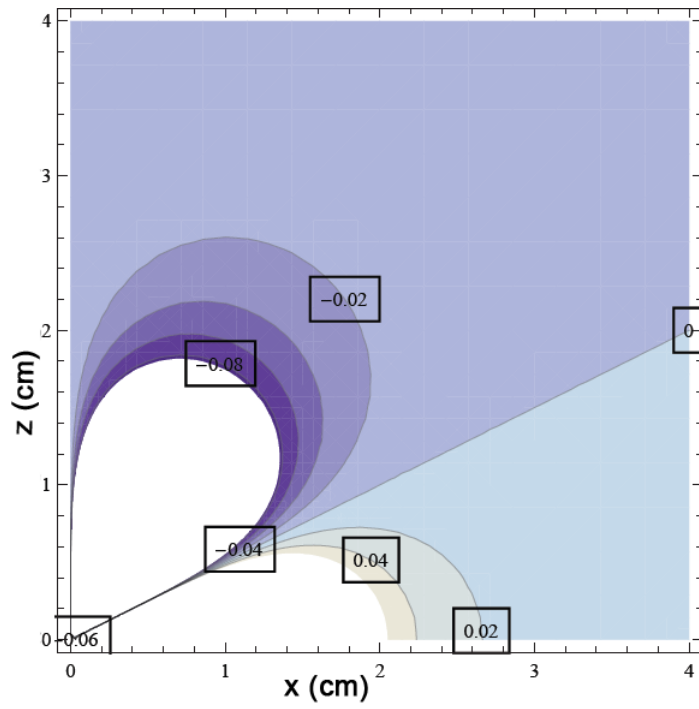


Figure 3.4: Contours for g_z for $\phi = 0^\circ$ and $0 \leq \theta \leq 90^\circ$.

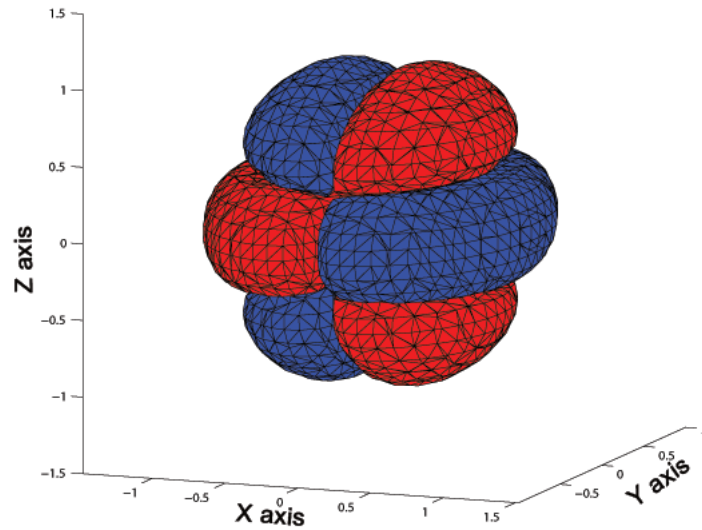


Figure 3.5: Contour for g_k presenting surfaces with $g_k = 0.5$ in blue and $g_k = -0.5$ in red. (This figure is best viewed in color).

Learning from figure 3.4 each coil will have 1 cm diameter and 1 cm height. They will be placed at ± 2 cm along x -axis. This will ensure that each coil is completely in a region with constant sign for g_k . Figure 3.6 shows the schematic for this coil configuration.

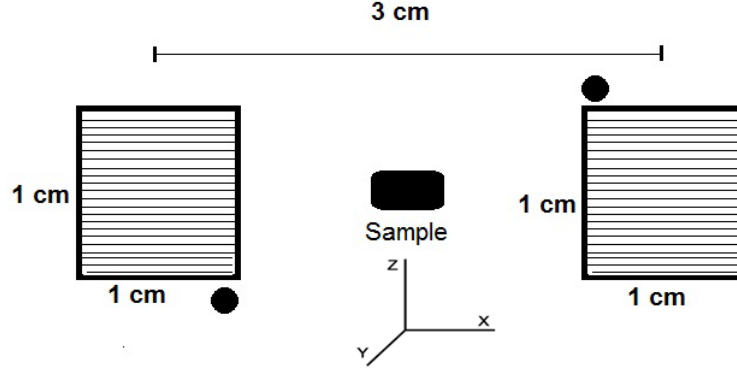


Figure 3.6: Schematic of detection coils. Dots show that both have opposite sense of winding

Then using equation 3.6 the voltage induced across this coil arrangement will be

$$V = 2\left(-\frac{3}{4\pi}m\mu_0\omega_0 \cos(\omega_0 t)d \sum_n \int_A dA \frac{x(r^2 - 5z^2)}{r^7}\right)$$

$$V = -\frac{3}{2\pi}m\mu_0\omega_0 \cos(\omega_0 t)\alpha d \quad (3.7)$$

where $\alpha = \sum_n \int_A dA \frac{x(r^2 - 5z^2)}{r^7}$.

3.3 Magnetization from Induced Voltage

The factor α in the expression for V only depends on the dimensions of the coils and is a constant for our coil arrangement. For calculating factor α assume the detection coil centered at $(2, 0, 0)$. Each turn of the coil is like a circular disk placed at $(2, 0, z)$ where z is the height of each turn. Integrating g_z over every circular disk and summing it up would give α . By symmetry the coil placed at $(-2, 0, 0)$ will have same α . The matlab file for calculating alpha is given in the appendix. The coils which were constructed for this project had 91 turns each, which gives $\alpha = 16.5118$.

From equation 3.7 the amplitude of induced voltage is given by

$$|V| = \frac{3}{2\pi}m\mu_0\omega_0\alpha d$$

which upon rearrangement gives,

$$m = \frac{2\pi V}{3\mu_0\omega_0\alpha d} \quad (3.8)$$

Hence we will attempt to investigate the magnetization m of the sample based upon equation 3.8.

Chapter 4

Construction and Characterization

So far we have discussed the details of vibration and detection mechanisms and based on these, selected a suitable detection coil configuration. Furthermore from the voltage induced in detection coils we can now work out the magnetization of the sample. In this chapter the practical implementation of the VSM will be discussed with details of mechanical and electrical components. Finally, the VSM will be tested on a few samples and the results will be analyzed. A complete schematic for our VSM is provided in Figure 4.1.

4.1 Construction

To provide the required magnetic field, an electromagnet (GMW model 3470) is used. For continuous operation it has a maximum input power of 0.11 kW (3.5 A/ 31 V). This limit is imposed by the resistive heating of the electromagnet coils. However the electromagnet can be water-cooled, with water cooling the maximum input power can be safely increased to 0.22 kW (5 A/ 44 V). Each pole piece of the electromagnet has a 40 mm diameter which tapers off to 20 mm pole face as shown in the figure 4.4. The maximum magnetic field that can be achieved under the input power limits, critically depends on the distance between the poles, the *pole gap*.

A bipolar operational power supply (KEPCO BOP 50-8D) is utilized to provide the current for the electromagnet. The power supply acts as a constant current source for the electromagnet. It can provide current from -8 A to 8 A and can be controlled directly from its front panel as well as remotely from any computer. The remote control is achieved by providing a voltage to the *current programming input* on the front panel of the power supply. This voltage is called the *control voltage*. The control voltage is simulated in a LabView file (Figure 4.10) and then generated by a DAQ (NI USB-6229) after which it is applied to the current programming input of the power supply. As the control voltage is linearly increased from -10 V to 10 V, the output current linearly increases from -8 A to 8 A.

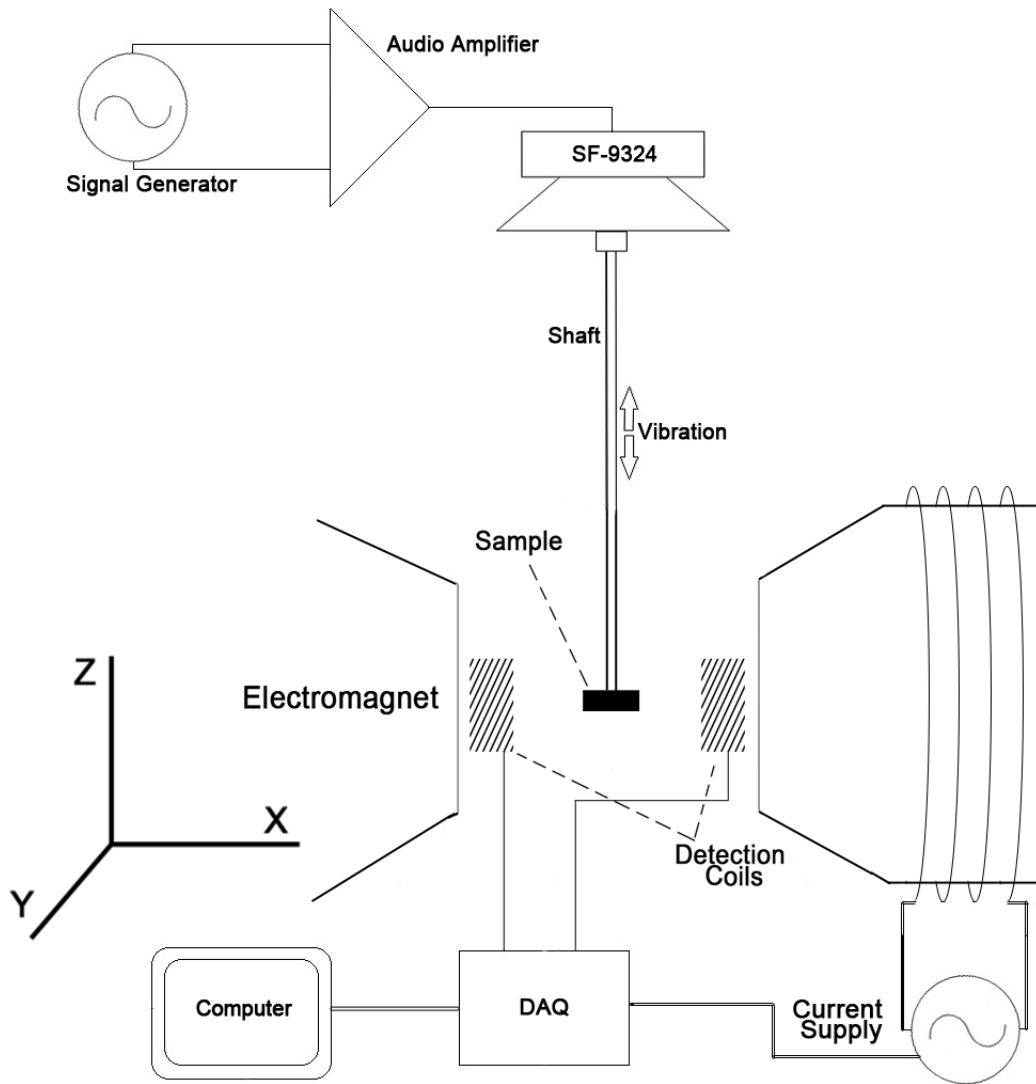


Figure 4.1: Schematic for the complete VSM.

The magnetic field generated at the center of the pole gap depends on the current provided to the electromagnet and the pole gap itself. With 40 mm pole gap the magnetic field at the center as a function of input current is shown in figure 4.2. The magnetic field was measured using a gauss meter (LakeShore 410) with a precision of 0.01 kG. The graph shows a linear relation between the input current and the resulting magnetic field. However a deviation from this relationship is seen after 6 A. If this limit is not crossed, the magnetic field at the center of the pole gap is directly proportional to the electromagnet current. Therefore we can use the input current as a measure of the magnetic field itself using a conversion factor of 0.49 ± 0.01 kG/A.

The pole pieces are made of soft iron. Their hysteresis plot is shown in figure 4.3 which indicates a maximum width of 20.4 Gauss at $I = 0$. The magnetic field was measured at the center of the pole gap using the gauss meter (LakeShore 410). The current was tuned from the controls provided on the front panel of the power supply.

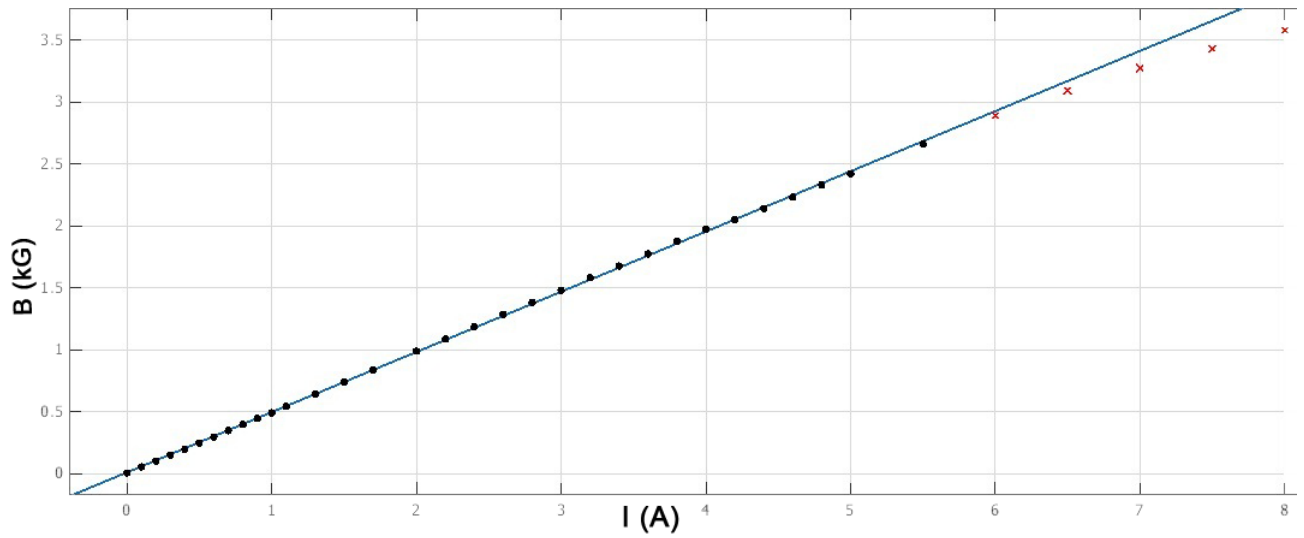


Figure 4.2: Calibration curve for the electromagnet. The slope provides a conversion factor of 0.49 kG/A valid up to 6 ampere current.

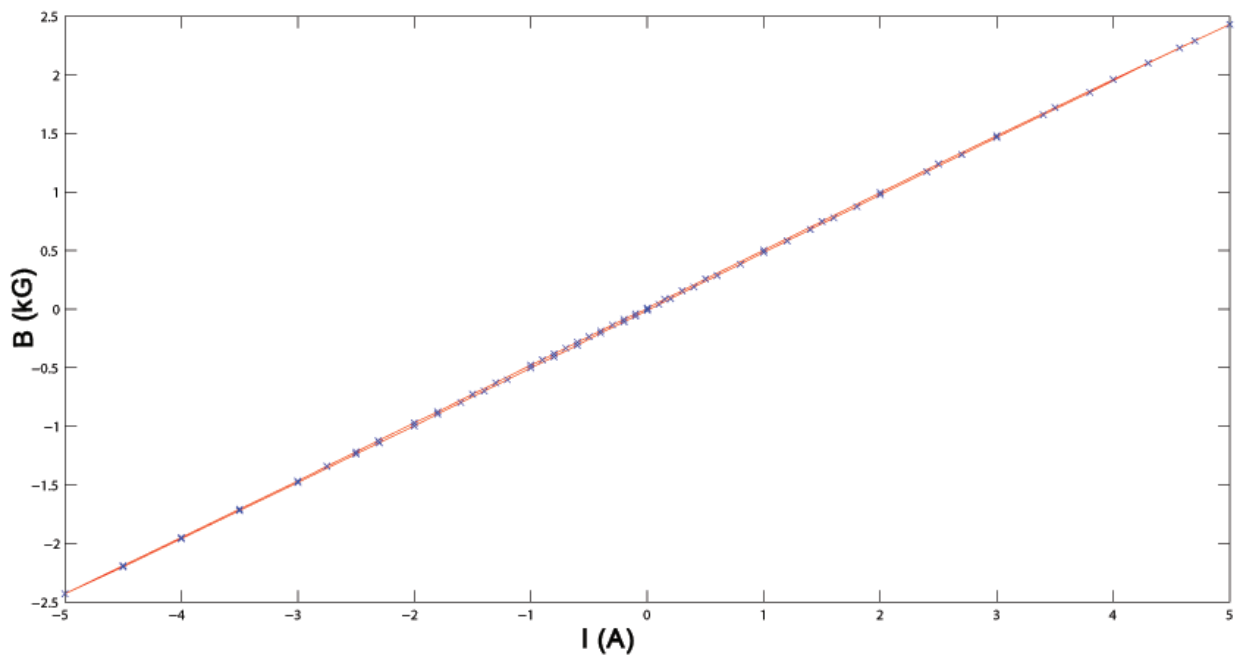


Figure 4.3: The hysteresis plot for the pole pieces of the electromagnet. It has a maximum width of 20.4 Gauss at $I = 0$

The detection coils are two single-layered coils, each being 1 cm in diameter and 1 cm in height. The assembly is drawn in figure 4.4. Both are wound by hand on a hollow paper core using a 0.09 mm thick copper wire. One is wound in the clockwise and the other in the anti-clockwise sense. Their resistance is measured by a simple multi-meter and their induction is observed using a digital inductance meter. Their specifications are summarized in table 4.1. The two coils are then secured in a wooden block with a center to center distance of 3 cm. In between

the two coils a cavity is carved out of the wooden block to provide space for the sample to vibrate. From one end to the other this assembly is 4 cm in length along the x -axis. As a result, a bare minimum gap of 4 cm is introduced between the poles of the electromagnet. This setup is shown in figure 4.5

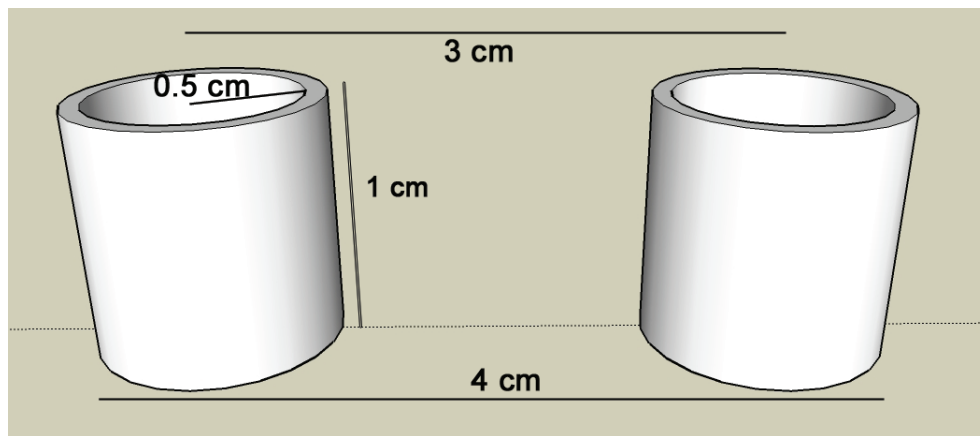


Figure 4.4: A sketch for the detection coil assembly.

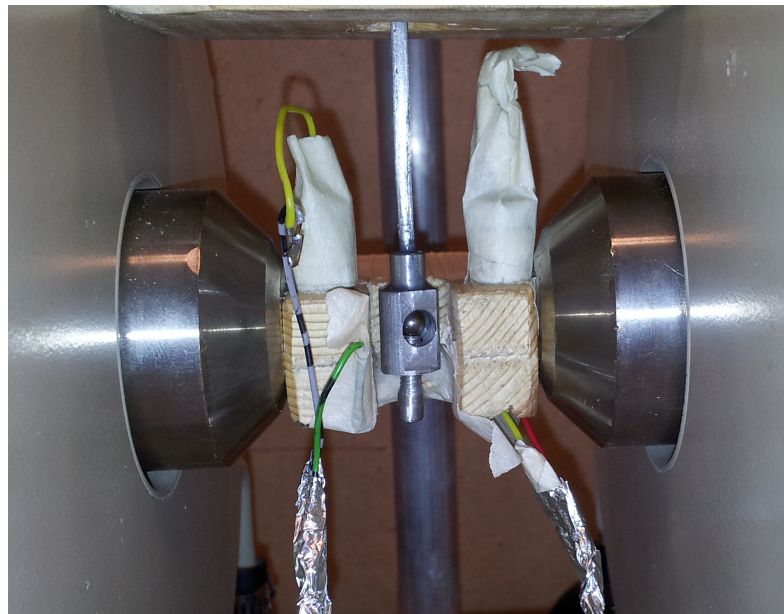


Figure 4.5: Detection coils in wooden block held between the poles of the electromagnet. In between the two coils is the sample placed inside the sample holder.

With the electromagnet placed as shown in figure 4.1, the magnetic field is generated in the horizontal direction and the sample is vibrated along the vertical direction at the center of the pole gap. This is achieved by mounting the vibrator over the electromagnet using a post. The vibrator is basically a speaker which is sensitive to external magnetic fields. To keep it safe from the fringing magnetic field of the electromagnet we have provided sufficient distance between the electromagnet and the vibrator. The sample is held in a nonmagnetic holder made from

Table 4.1: Specifications of detection coils

Property	Coil 1	Coil2
Resistance (Ω)	106 ± 1	104 ± 1
Number of turns	91	91
Inductance (μH)	62.3 ± 0.1	62.3 ± 0.1
Wire diameter (mm)	0.09 ± 0.01	0.09 ± 0.01
Height (cm)	1 ± 0.01	1 ± 0.01
Diameter (cm)	1 ± 0.01	1 ± 0.01

Table 4.2: Elemental Composition of the iron strip sample

Element	Percentage
Iron	90
Cobalt	6-7
Molybdenum	0.97
Chromium	0.75
Nickel	0.64

aluminium and attached to the vibrator using an aluminium shaft which extends the sample safely into the magnetic field of the electromagnet. The shaft, the vibrator and the sample holder are connected to each other by threading. This structure is shown in figure 4.6.

For holding spherical and flat samples, two different sample holders are made. In both of them the sample is placed in a cavity and held fixed by an aluminium screw. These assemblies are shown in figure 4.7. The mechanical assembly was built in the Physlab workshop.

The voltage signal generated in the coils was sent to LabView software by a DAQ (NI USB 6229) interface, where it was filtered and recorded.

4.2 Experimentation

For testing the VSM, a 4 mm diameter ball-bearing and a 7.3×6.4 mm strip of iron were used as the two test samples. The iron strip was cut out of a core plate extracted from a transformer. X-ray fluorescence spectroscopy showed that it contained 90 % iron. The complete elemental composition is summarized in table 4.2. In the X-ray fluorescence spectroscopy, X-rays are shined upon the sample. As a result, different elements present in the sample give off their characteristic X-ray radiations which are then utilized to determine the elemental composition of the sample. High iron percentage indicates a soft magnetic nature for the iron strip sample i.e. it will show little hysteresis.

The ball-bearing sample is vibrated at 100 Hz with a mechanical amplitude of 0.5 mm. The induced voltage is shown in figure 4.8. Since the sample is vibrated sinusoidal, a sinusoidal signal should be induced in the coils. Furthermore increasing the applied magnetic field should increase the magnetization of the sample

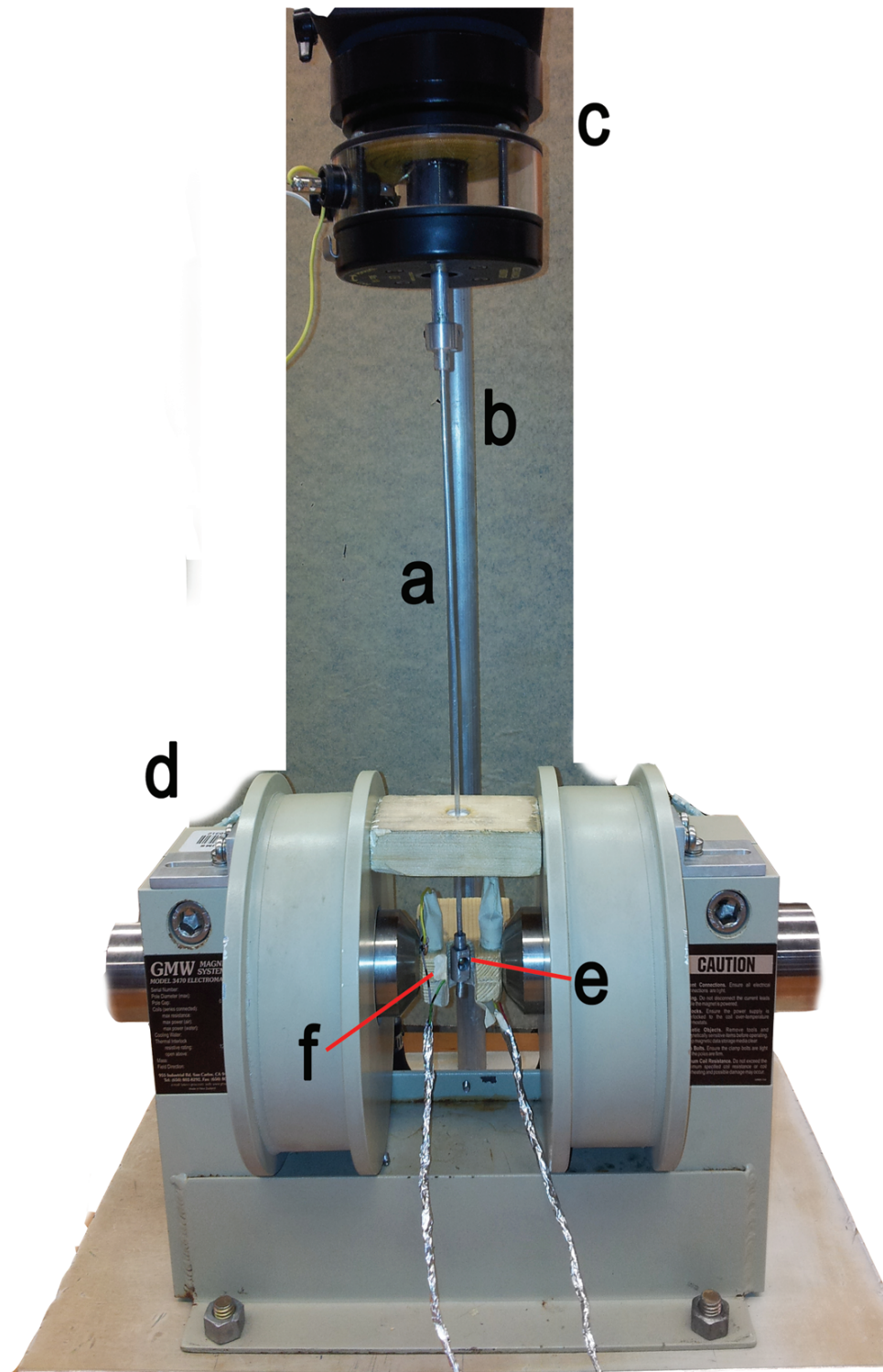


Figure 4.6: Mechanical structure of VSM showing (a) extension rod, (b) holding post (c) vibrator (d) electromagnet, (e) sample holder with a ball-bearing as sample and (f) detection coil.

which should result in an increase in the induced voltage. Both these artifacts can be clearly seen in the figure 4.8. The magnetization calculated from the induced voltage using equation 3.8 is summarized in table 4.3

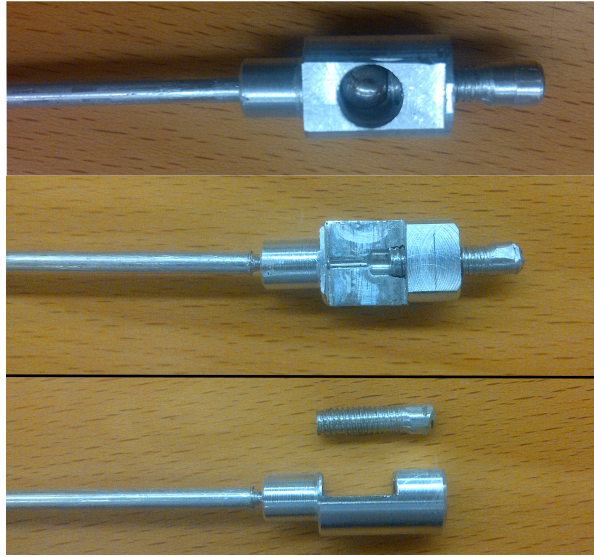


Figure 4.7: Aluminium sample holders for holding samples in VSM

Table 4.3: Magnetization of the ball-bearing sample

Applied field (kG)	Magnetization (A/m)
0.00	3.14
0.49	37.0
0.97	77.8
1.94	155
2.43	207

It was observed that the magnetized sample experiences a considerable force due to the external magnetic field. This results in bending of the extension rod. To prevent this the extension rod was passed through a teflon ring mounted in a wooden block fixed on the electromagnet. It can be seen in figure 4.6 above the detection coils.

To observe the magnetic hysteresis of the sample the electromagnet power supply is remotely controlled from a computer. For this purpose a LabView file is constructed which is shown in figure 4.10. It controls the electromagnet current and tunes the magnetic field linearly in a programable number of steps and time. With an additional command structure, shown in figure 4.9, the same LabView file is utilized to record the induced voltage as well. The induced voltage is converted to magnetization of the sample using equation 3.8. If all terms are in SI units then the magnetization is given in ampere per meter by equation 3.8.

The hysteresis loop for ball-bearing vibrated at 100 Hz with 0.5 mm mechanical amplitude is shown in figure 4.11. The induced voltage was measured continuously at a sample rate of 1 kHz with strength range of $\pm 10\text{mV}$ by LabView-DAQ interface and the applied magnetic field was tuned within $\pm 2.93\text{ kG}$ in 200 steps. Therefore the loop appears stair-shaped. However we can make it smooth by choosing more number of smaller steps. The voltage readings were converted to the magnetization of the sample using equation 3.8.

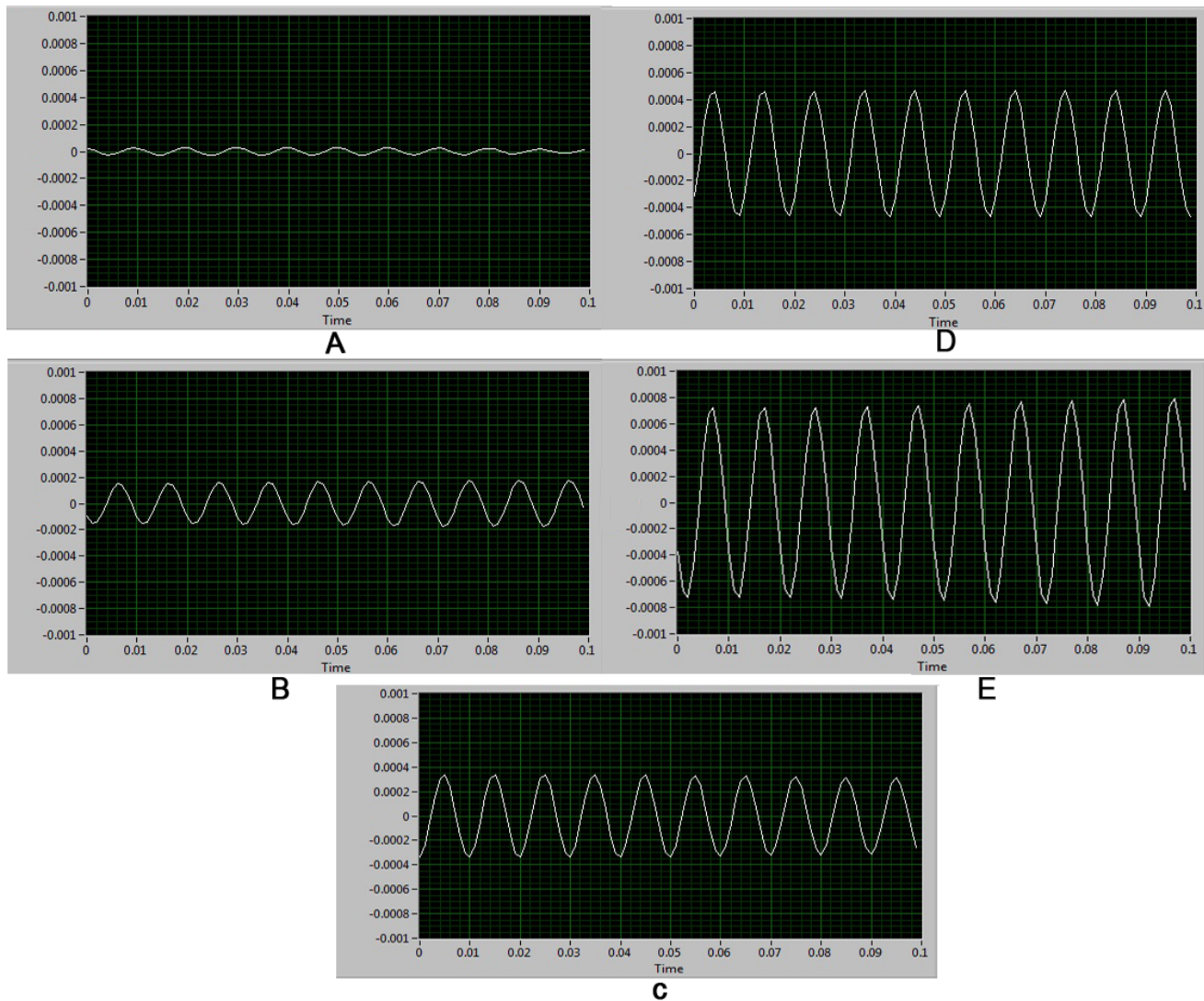


Figure 4.8: Voltage induced in the detection coils. The horizontal axis mark time in seconds and voltage is give along vertical axis in volts. The magnetic field is increased from (A) through (E). Applied magnetic fields are (A) 0 kG, (B) 0.49 kG (C) 0.97 kG, (D) 1.94 kG and (E) 2.43 kG.

The hysteresis loop has a very small thickness indicating soft magnetic nature of the ball-bearing sample. Furthermore the hysteresis of the pole pieces also plays a roll in this loop. The slope is almost constant throughout the loop which indicates that saturation is not achievable within the applied magnetic field limits.

The hysteresis loop for the metal strip sample is shown in figure 4.12. Just like the ball-bearing sample, it is vibrated at 100 Hz with mechanical amplitude of 0.5 mm. The LabView settings are the same, except that this time a smaller step size is introduced and the number of steps have been increased to 400. This has made it smoother than the one for the ball-bearing sample. From the thin width of the loop it is clear that the metal strip too has a soft magnetic nature. However a trend towards the saturation magnetization is now clearly observable. Slight irregularities can be observed at the ends of the loop which are consequence of

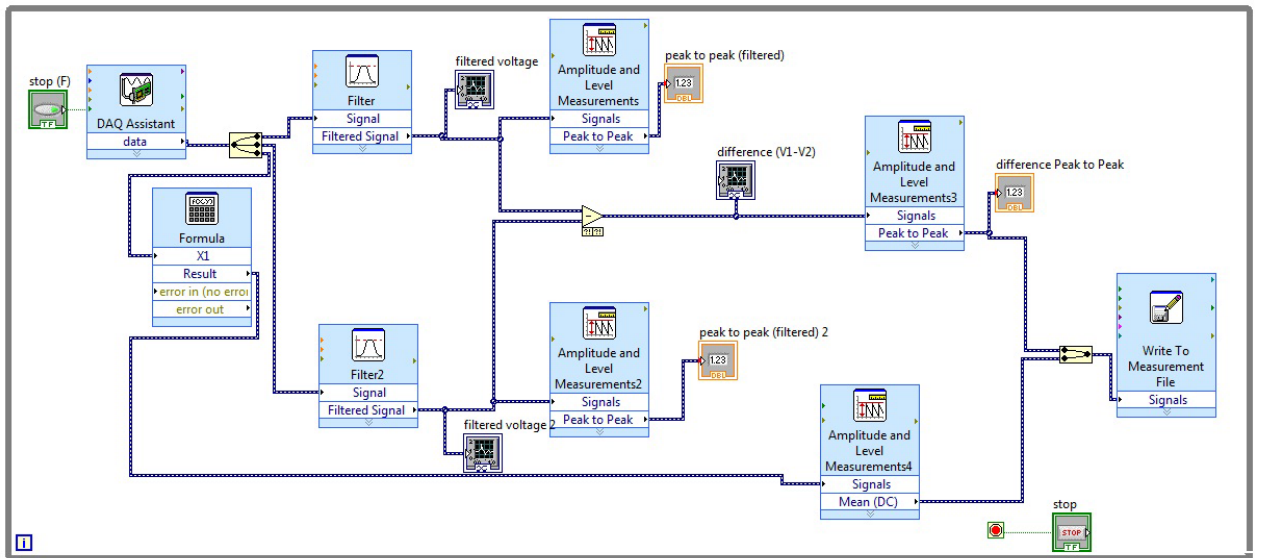


Figure 4.9: Block diagram for LabView file used to acquire voltage induced in detection coils.

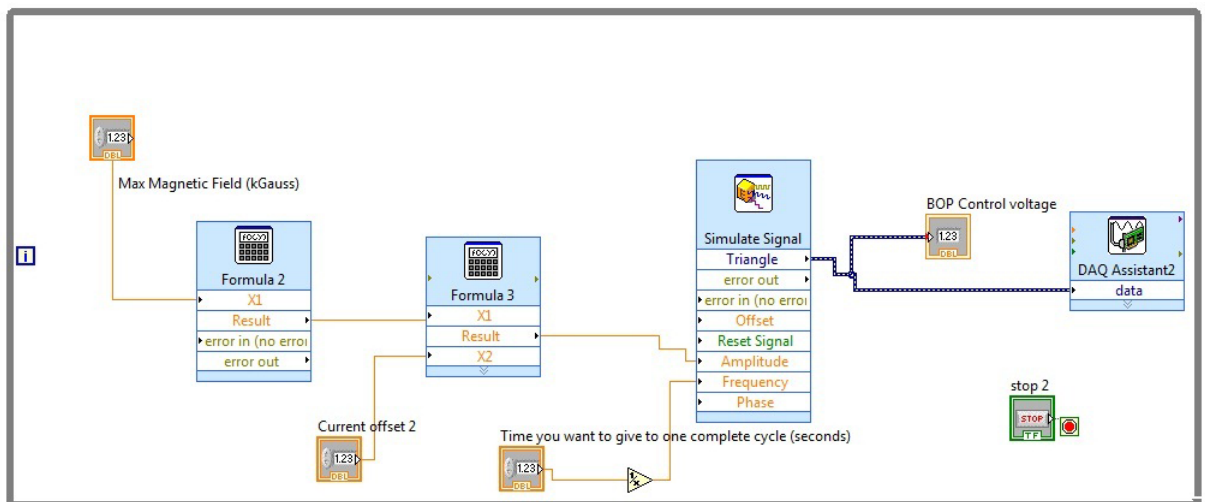


Figure 4.10: Block diagram of control loop used to operate the current source for the electromagnet.

unwanted mechanical vibrations in the mechanical structure of the VSM.

A small pellet of ferri magnetic substance (Fe_3O_4) is also tested. However due to limited sensitivity of the VSM only a small voltage is observed even at maximum magnetic field of 3.58 kG (figure 4.13). It is observed that changing the sensitivity of the LabView-DAQ interface does not improve the observed signal. A possible solution could be to employ an instrumentation amplifier to magnify the signal before it is fed to the DAQ.

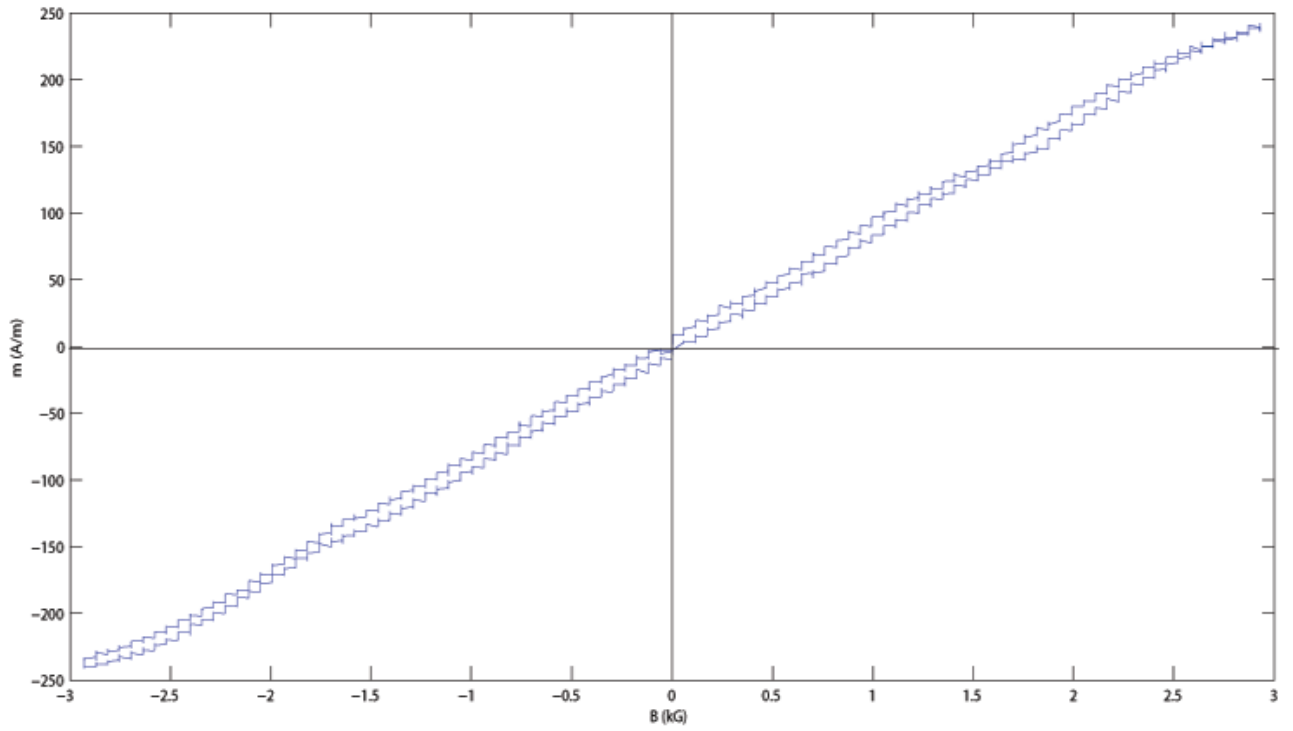


Figure 4.11: Hysteresis loop for the 4 mm ball-bearing.

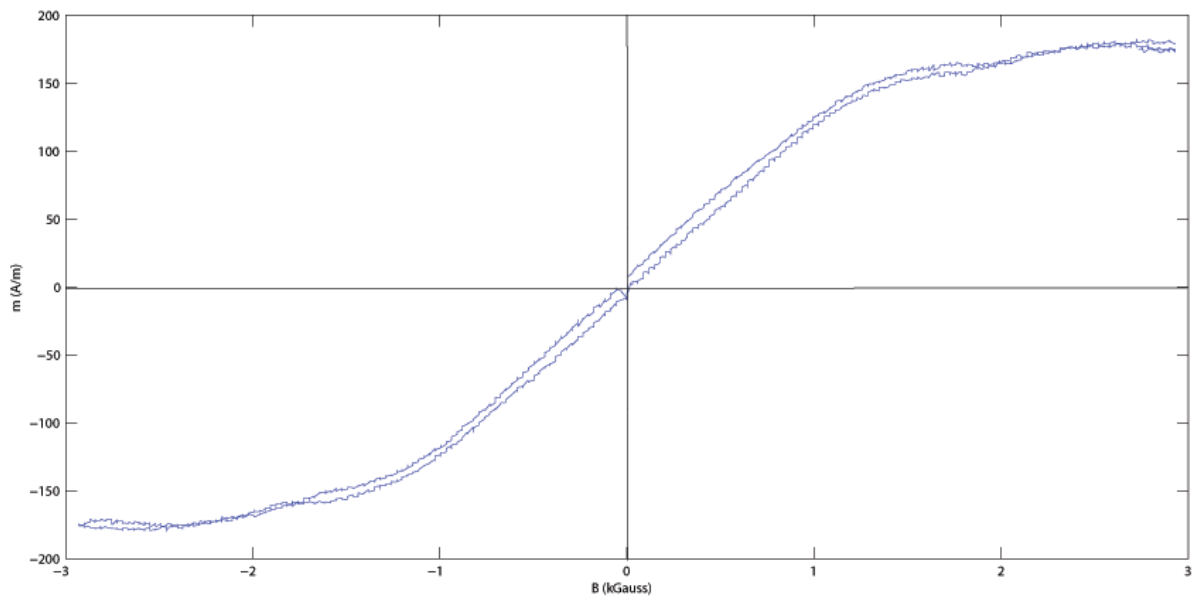


Figure 4.12: Hysteresis loop for the 7.3×6.4 mm strip of iron.

4.3 Conclusion

The experimental analysis so far suggests that our VSM works in principle. Its performance for ferro-magnetic samples with considerable size is satisfactory. We are able to see most of the qualitative and some of the quantitative aspects of

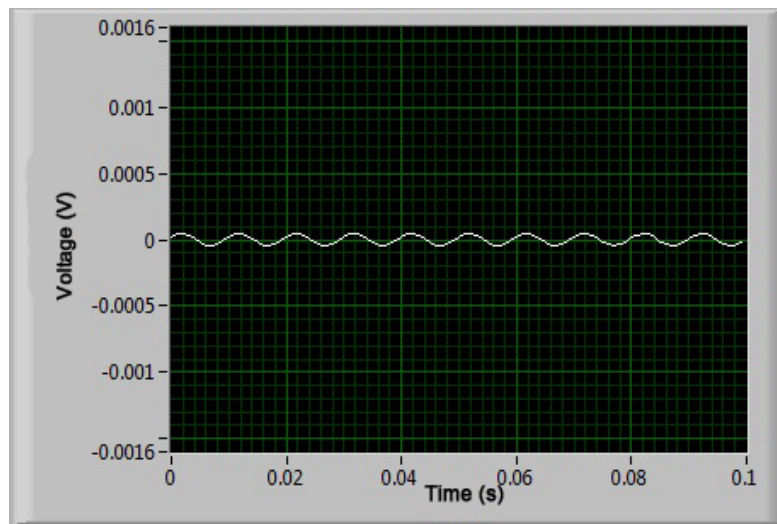


Figure 4.13: Voltage observed for Fe_3O_4 pellet at maximum magnetic field.

different samples clearly. However we need to test the validity of the results. This can be achieved by using a sample of known magnetization and then calculating its magnetization using our VSM.

For weakly magnetic substances, the performance of the VSM is not satisfactory. To measure the magnetization of such samples, the sensitivity of VSM needs to be improved. Furthermore since the sample is vibrated at a particular frequency, a lock-in amplifier can be used in future to measure the induced voltage for weakly magnetic samples.

Bibliography

- [1] B. D. Culity, C. D. Graham *Introduction to Magnetic Materials* 2009: Wiley-Interscience.
- [2] David S. Nyce *Linear Position Sensors, Theory and Application* 2004: Wiley-Interscience.
- [3] Gene F. Franklin, J. David Powell, Abbas Emami-Naeini *Feedback Control of Dynamic Systems* 2006: Pearson Prentice Hall.
- [4] G. J. Bowden *Detection Coil System for Vibrating Sample Magnetometers* 1972: CSIRO Division of Applied Physics, National Standards Laboratory, University Grounds, Chippendale, NSW, 2008, Australia.
- [5] David Jiles *Introduction to Magnetism and Magnetic Materials* 1998: CRC press.
- [6] www.mathworks.com/help/curvefit/cftool.html

Appendix

```
%% consider a coil of hight 'h', radius 0.5 ,placed at x=2, y=0
% each turn of coil acts as a circular patch of area center at x=2,y=0 and
% it's hight is given by z. For n number of turns the hights are incoded in
% the array z below. Now for finding alpha we simply sum up the integrals
% of g_k over all turns of coil. This summation is performed in the loop
% below.
clc;clear all
n = 91;
z = -0.5:1/n:0.5;
alpha = 0;
for i = 1:length(z)
    fun = @(r,theta) ((2+r.*cos(theta)).*((2+r.*cos(theta)).^2+...
    (r.*sin(theta)).^2-4*(z(i)).^2))./((2+r.*cos(theta)).^2+(r.*sin(theta)).^2+(z(i)).^2).^(7/2);
    q = integral2(fun,0,0.5,0,2*pi);
    alpha = alpha+q;
end
alpha
```

Figure 4.14: Code for finding α